

Figure 2. Wnt5a induces the expression of laminin γ 2 in GC cells. (A) *Wnt5a* and *LAMC2* mRNA expression in various GC cell lines was quantified by quantitative reverse-transcription PCR. Relative mRNA levels in each cell line were expressed as percentages of *Wnt5a* mRNA in MKN-1 cells and *LAMC2* mRNA in MKN-45 cells. The results shown are the means \pm SE of 3 independent experiments. (B) TMK-1 cells. (Left panel) *LAMC2* mRNA levels in TMK-1/control and TMK-1/*Wnt5a* KD cells were quantified. (Second panel) TMK-1 cells were treated with the indicated concentrations of *Wnt5a* (closed circles) or *Wnt3a* (open circles) for 4 hours, and then the *LAMC2* mRNA level was quantified. (Third panel) TMK-1 cells were treated with 100 ng/mL *Wnt5a* for the indicated periods, and then *LAMA3*, *LAMB3*, and *LAMC2* mRNA levels were quantified. (Right panel) TMK-1 cells were treated with 150 ng/mL *Wnt5a* or *Wnt3a* for 8 hours, and then extracellular matrix was collected and probed with anti-laminin α 3, β 3, and γ 2 antibodies. (C) MKN-1 cells. (Left panel) *LAMC2* mRNA levels in MKN-1 cells transfected transiently with scramble (control), *Wnt5a*, or *Wnt3a* siRNA were quantified. (Right panel) Total cell lysates of MKN-1 cells transfected transiently with scramble, *Wnt5a*, or *Wnt3a* siRNA were probed with anti-laminin γ 2 antibody. (D) MKN-45 cells. (Left panel) *LAMC2* mRNA levels in MKN-45/control and MKN-45/*Wnt5a* cells were quantified. Relative mRNA levels were expressed as fold increases compared with the *LAMC2* mRNA level in MKN-45/control cells. (Right panel) Extracellular matrix prepared from MKN-45/control and MKN-45/*Wnt5a* cells was probed with anti-laminin γ 2 antibody. Laminin γ 2' is a 105-kilodalton processed form of laminin γ 2.

Wnt5a and *Wnt3a* proteins were added to TMK-1 cells, *Wnt5a* but not *Wnt3a* increased *LAMC2* mRNA in a dose-dependent manner (Figure 2B). *LAMC2* mRNA started to increase at 2 hours after *Wnt5a* stimulation, reached a maximal level at 4 hours, and then declined gradually (Figure 2B). Laminin-5 is a trimmer of lami-

nin α 3, β 3, and γ 2 chains. mRNA levels of other components of laminin-5, *LAMA3* (*laminin α 3* gene) and *LAMB3* (*laminin β 3* gene), were not up-regulated by *Wnt5a* (Figure 2B). Consistent with these results, *Wnt5a* increased protein levels of laminin γ 2 but not laminin α 3 and laminin β 3 (Figure 2B).

Knockdown of Wnt3a from MKN-1 cells did not affect *LAMC2* mRNA and laminin $\gamma 2$ protein levels under conditions where knockdown of Wnt5a reduced them (Figure 2C). MKN-45 cells stably overexpressing Wnt5a (MKN-45/Wnt5a cells) increased the expression of *LAMC2* mRNA and laminin $\gamma 2$ protein as compared with control cells (Figure 2D). Taken together, these

results indicate that Wnt5a induces the expression of laminin $\gamma 2$ in 3 different GC cell lines.

Wnt5a Activates the Promoter of Laminin $\gamma 2$ Through the AP-1 Element

To examine how Wnt5a signaling induces the expression of laminin $\gamma 2$, TMK-1 cells were pretreated

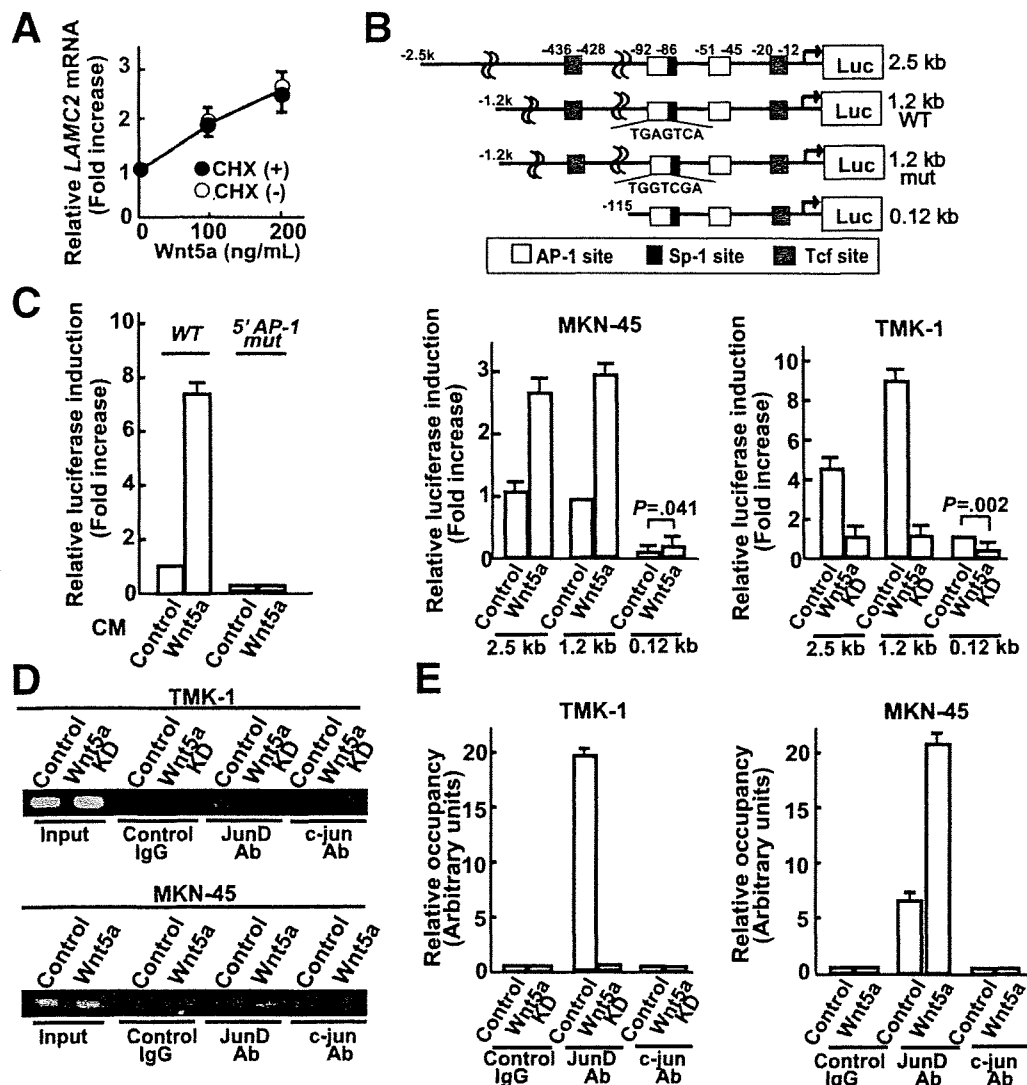


Figure 3. AP-1 is involved in Wnt5a-dependent expression of laminin $\gamma 2$. (A) TMK-1 cells were treated with (closed circles) or without (open circles) 1 μ g/mL cycloheximide (CHX) for 4 hours before stimulation with the indicated amounts of Wnt5a for 4 hours. *LAMC2* mRNA was quantified, and relative mRNA levels were expressed as fold increases compared with the *LAMC2* mRNA level in TMK-1 cells without Wnt5a stimulation. (B) (Upper panel) The *LAMC2*-luciferase constructs used in this study. (Bottom left panel) MKN-45/control or MKN-45/Wnt5a cells were transfected with the indicated pGL3/*LAMC2*-Luc constructs, and then the luciferase activities were measured. (Bottom right panel) TMK-1/control or TMK-1/Wnt5a KD cells were transfected with the indicated pGL3/*LAMC2*-Luc constructs, and then the luciferase activities were measured. Relative laminin $\gamma 2$ promoter activity was expressed as fold increase compared with that of MKN-45/control cells transfected with pGL3/(1.2 kb) *LAMC2*-Luc or TMK-1/control cells transfected with pGL3/(0.12 kb) *LAMC2*-Luc. (C) After TMK-1 cells were transfected with pGL3/(1.2 kb) *LAMC2*-Luc with or without mutation in the 5' AP-1 site (5' AP-1 mut or WT, respectively), the cells were stimulated with control CM or Wnt5a CM for 24 hours. Luciferase activities were measured and expressed as fold increases compared with that of cells transfected with pGL3/(1.2 kb) *LAMC2*-Luc and treated with control CM. WT, wild type. (D) Chromatin from TMK-1/control, TMK-1/Wnt5a KD, MKN-45/control, and MKN-45/Wnt5a cells was immunoprecipitated with anti-JunD antibody, anti-c-jun antibody, or control immunoglobulin G, and the samples were analyzed by PCR for the *LAMC2* promoter region containing 2 AP-1 sites. (E) The amounts of precipitated DNA in D were quantified by real-time PCR with the same primers. The relative amounts of the DNA fragments containing AP-1 sites immunoprecipitated with anti-JunD or anti-c-jun antibody were expressed as arbitrary units compared with that with control immunoglobulin G. The results shown are means \pm SE from 3 independent experiments.

with cycloheximide before Wnt5a stimulation. Cycloheximide did not affect Wnt5a-dependent expression of *LAMC2* mRNA (Figure 3A), suggesting that Wnt5a induces the expression of *LAMC2* mRNA without protein synthesis.

To evaluate the role of the upstream elements in controlling basal activity of the *LAMC2* promoter, a series of deletions of the *LAMC2* 5'-flanking region with the luciferase gene (*LAMC2-Luc*) was transfected into MKN-45/control cells. Consistent with previous observations in colon cancer cells,¹⁹ the 2.5-kilobase (kb) and 1.2-kb *LAMC2-Luc* constructs showed luciferase activity, but deletion from position -1.2 kb to -0.12 kb reduced the luciferase activity to 10% (Figure 3B). Similar findings were observed in TMK-1 cells (Figure 3B). When 3 different *LAMC2-Luc* constructs were transfected into MKN-45/Wnt5a cells, the luciferase activity increased approximately 3-fold as compared with the control cells (Figure 3B). When Wnt5a was knocked down from TMK-1 cells, the *LAMC2-Luc* promoter activities were decreased (Figure 3B). These results suggest that the region between -1.2 kb and -0.12 kb was required for the basal activity of the *LAMC2* promoter and that the -0.12 kb region has a Wnt5a response element.

It has been reported that the 0.12-kb promoter fragment contains 2 AP-1 elements and that the 5' AP-1 site is critical for phorbol ester-dependent activation.¹⁹ As shown in Figure 3C, the basal reporter gene activity was decreased dramatically by introducing mutations in this area (*LAMC2(5'AP-1 mut)-Luc*), and Wnt5a did not stimulate it. Therefore, the 5' AP-1 site could be crucial for the basal activity of the *LAMC2* promoter as well as the upstream region.

The AP-1 protein containing JunD has been shown to bind to the 5' AP-1 site in the *LAMC2* promoter using electrophoretic mobility shift assays.¹⁹ In ChIP assays,

PCR amplification of the anti-JunD antibody immunoprecipitants showed that the fragment of the *LAMC2* promoter containing 2 AP-1 sites exists in TMK-1/control cells but not in TMK-1/Wnt5a KD cells (Figure 3D and E). PCR using the fragment containing a T-cell factor (Tcf) binding site, which is located about 400 base pairs upstream of the AP-1 sites, showed no detectable bands in both samples (data not shown). In addition, the PCR fragment of the *LAMC2* promoter containing AP-1 sites in the anti-JunD antibody immunoprecipitants was increased in MKN-45/Wnt5a cells (Figure 3D and E). However, anti-c-jun antibody did not immunoprecipitate the PCR fragment (Figure 3D and E).

We also examined which molecules are involved in Wnt5a-dependent expression of laminin γ 2. Consistent with previous results in other cells,^{7,8,20} Wnt5a induced the phosphorylation of c-Jun-N-terminal kinase (JNK) and PKC α in MKN-45 and TMK-1 cells (Figure 4A), indicating the activation of JNK and PKC α . SP600125, a JNK inhibitor, and staurosporine, a PKC inhibitor, suppressed Wnt5a-dependent *LAMC2-Luc* activity (Figure 4B). Frizzled (Fz) family are known to function as Wnt receptors.²¹ Fz2, Fz5, and Fz7 were expressed highly in MKN-1 cells (data not shown). Knockdown of Fz2 but not of Fz5 and Fz7 reduced Wnt5a-dependent expression of *LAMC2* mRNA (Figure 4C). Taken together, these results suggest that Fz2 is a Wnt5a receptor in this signaling of GC cells and that JNK and PKC mediate Wnt5a-dependent expression of laminin γ 2 through the recruitment of JunD to the AP-1 site of the *LAMC2* promoter.

Laminin γ 2 Mediates Wnt5a-Dependent Invasion

It has been reported that β -catenin activates *LAMC2* promoter function through 2 Tcf-binding ele-

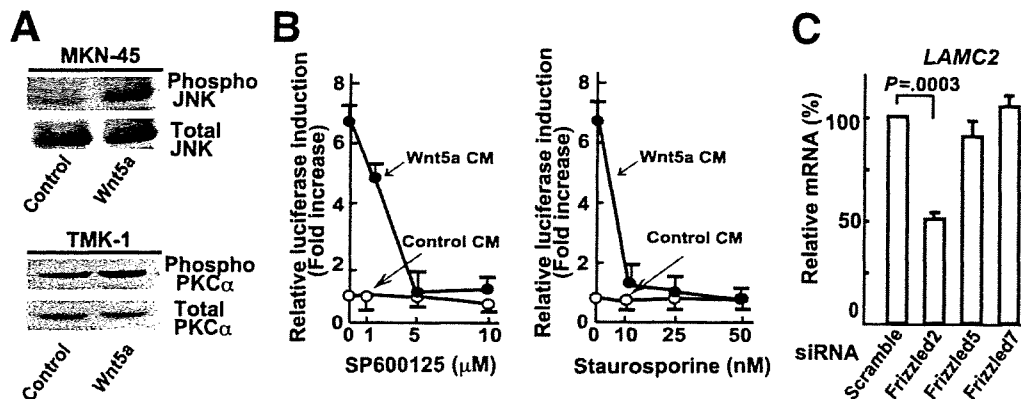


Figure 4. The mechanism by which Wnt5a induces the expression of laminin γ 2. (A) MKN-45 cells were stimulated with 300 ng/mL Wnt5a for 1 hour, and then the cell lysates were probed with anti-phospho-JNK antibody. TMK-1 cells were stimulated with 300 ng/mL Wnt5a for 30 minutes, and then the cell lysates were probed with anti-phospho-PKC α antibody. (B) After TMK-1 cells were transfected with pGL3/(1.2 kb) *LAMC2-Luc*, the cells were stimulated with control (open circles) or Wnt5a (closed circles) CM for 24 hours in the presence of the indicated concentrations of SP600125 (left panel) or staurosporine (right panel). Luciferase activities were measured and expressed as fold increases compared with that of cells treated with control CM and without inhibitors. (C) After MKN-1 cells were transfected with the indicated siRNA, *LAMC2* mRNA levels were quantified.

ments, suggesting that laminin $\gamma 2$ mediates β -catenin-dependent invasion by colon cancer cells.²² Therefore, the possibility that β -catenin mediates Wnt5a-dependent expression of laminin $\gamma 2$ was examined, because Wnt5a can activate the β -catenin-dependent pathway in a receptor context.²³ Expression of β -catenin and Tcf-4 in TMK-1 cells stimulated the promoter activity of *LAMC2*, but the activity was not affected by SP600125 (Figure 5A). Laminin $\gamma 2$ protein levels were also increased by the expression of β -catenin and Tcf-4, although the increment was slight compared with the extent induced by Wnt5a stimulation but reproducible (Figure 5B). Δ Tcf-4, which lacks the β -catenin-binding region, is known to act as a dominant negative form.²⁴ Δ Tcf-4 did not affect the Wnt5a-dependent promoter activity of *LAMC2* (Figure 5A). Fur-

thermore, Wnt5a and β -catenin stimulated the promoter activity of *LAMC2* additively (Figure 5A). These results suggest that Wnt5a induces the expression of laminin $\gamma 2$ without the activation of the β -catenin-dependent pathway.

Knockdown of laminin $\gamma 2$ in TMK-1 and MKN-1 cells clearly decreased invasion activities in the Transwell assays with Matrigel (Figure 5C). Furthermore, MKN-45/Wnt5a cells showed higher invasion activity compared with control cells, and knockdown of laminin $\gamma 2$ decreased the activity (Figure 5C). Consistent with these observations, laminin $\gamma 2$ was clearly expressed in TMK-1 cells metastasized to liver in nude mice (Figure 5D). Taken together, these results suggest that Wnt5a is involved in the expression of laminin $\gamma 2$, which mediates Wnt5a-dependent invasion at least partly in a certain type of GC.

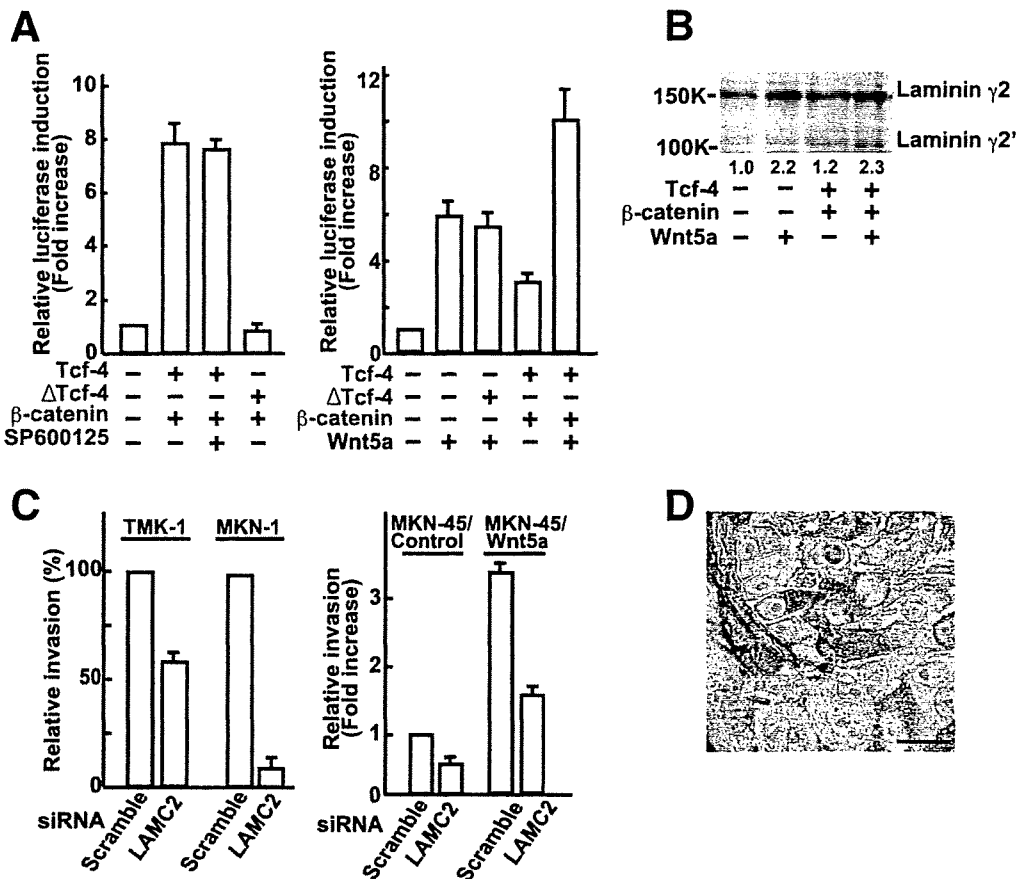


Figure 5. Laminin $\gamma 2$ mediates Wnt5a-dependent cell invasion. (A) (Left panel) TMK-1 cells were transfected with pGL3/(1.2 kb) *LAMC2-Luc* and the indicated plasmids in the presence or absence of 10 μ mol/L SP600125. At 48 hours after transfection, luciferase activities were measured. The relative laminin $\gamma 2$ promoter activity was expressed as fold increase compared with that of the cells transfected with empty vectors and without treatment of SP600125. (Right panel) At 24 hours after TMK-1 cells were transfected with pGL3/(1.2 kb) *LAMC2-Luc* and the indicated plasmids, the cells were stimulated with control CM or Wnt5a CM for 24 hours. The relative luciferase activities were expressed as fold increases compared with that of cells transfected with empty vectors and stimulated with control CM. (B) TMK-1 cells were transfected with plasmids for β -catenin and Tcf-4 and then stimulated with 150 ng/mL Wnt5a as indicated. The extracellular matrix fractions of all these samples were collected and probed with anti-laminin $\gamma 2$ antibody. The numbers below the panel show relative quantification values of laminin $\gamma 2$ in each lane. (C) (Left panel) TMK-1 and MKN-1 cells were transfected with scramble or *LAMC2* siRNA, and then the cells were subjected to the invasion assay. Relative invasion activity was expressed as percentages of the invaded cell numbers of control cells. (Right panel) MKN-45/control and MKN-45/Wnt5a cells were transfected transiently with scramble or *LAMC2* siRNA, and these cells were subjected to the invasion assay. Relative invasion activity was expressed as fold increase compared with the invaded cell numbers in MKN-45/control cells transfected with scramble siRNA. (D) Liver tumors produced by the intrasplenic injection of TMK-1 cells were sectioned and stained with anti-laminin $\gamma 2$ antibody. All the cells shown in this figure were metastasized GC cells. Laminin $\gamma 2$ was stained in brown. Scale bar = 19 μ m.

Coexpression of Wnt5a and Laminin γ 2 in GC Cases

To investigate the induction of laminin γ 2 expression by Wnt5a in GC cases, immunohistochemical analyses of Wnt5a and laminin γ 2 in 153 GC cases were performed. Representative results of Wnt5a immunostaining of GC are shown in Figure 6A and Supplementary Figure 2 (see supplemental material online at www.gastrojournal.org). Wnt5a was detected in the cytoplasm of cancer cells. Consistent with the previous observations,⁶ positivity for Wnt5a was associated with advanced T classification, N classification, and tumor stage (Supplementary Table 2).

Two laminin γ 2 staining patterns (extracellular staining and cytoplasmic staining) have been reported in

GC.¹⁵ In diffuse-scattered type (so-called scirrhous type) GC cases, cytoplasmic laminin γ 2 staining but not extracellular laminin γ 2 staining was found (Figure 6B and Supplementary Figure 2). In other types (intestinal or diffuse-adherent type) of GC cases, both staining patterns were observed (Figure 6C and D). Because Wnt5a staining was detected in few cancer cells in the GC cases with extracellular laminin γ 2 expression, the relationship between the expression of Wnt5a and cytoplasmic laminin γ 2 was investigated.

In total, 35 (23%) of 153 GC cases were recognized as cytoplasmic laminin γ 2 positive. Positivity for laminin γ 2 was associated with advanced N classification ($P = .0037$) and tumor stage ($P = .0330$) (Table 1). Among 36 diffuse-scattered type GC cases, the frequency of laminin γ 2

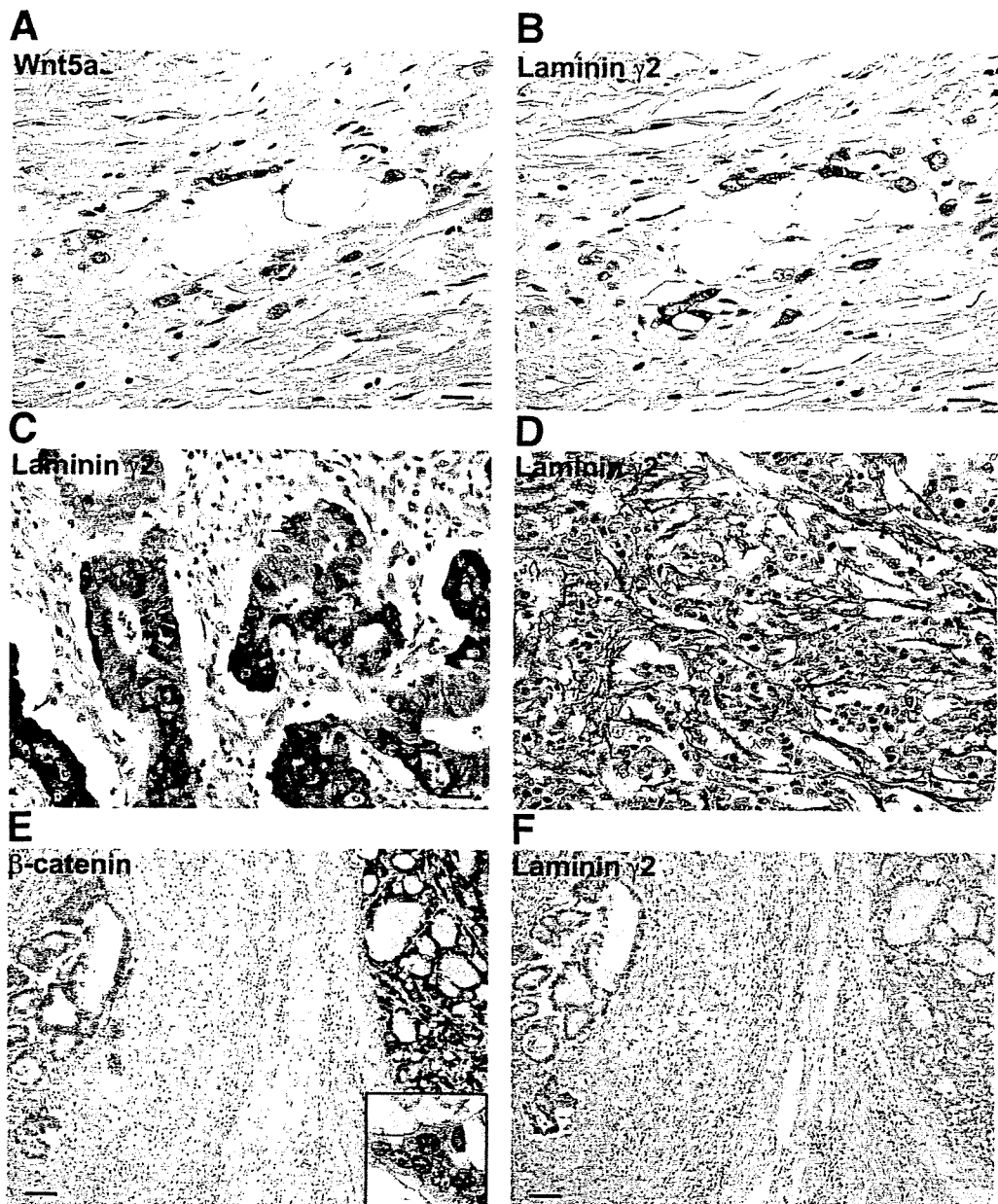


Figure 6. Coexpression of Wnt5a and laminin γ 2 in scirrhous GC. (A and B) A sample of diffuse-scattered type GC was stained with (A) anti-Wnt5a and (B) anti-laminin γ 2 antibodies. Cytoplasmic laminin γ 2 was detected in Wnt5a-positive cancer cells. Scale bars = 19 μ m. (C and D) Samples of other GC types were stained with anti-laminin γ 2 antibody. Laminin γ 2 was observed as (C) cytoplasmic expression in intestinal type GC and (D) extracellular expression in diffuse-adherent type GC patterns. Scale bars = 19 μ m. (E and F) A sample of GC was stained with (E) anti- β -catenin and (F) anti-laminin γ 2 antibodies. (Inset) High-magnification image of β -catenin staining. Scale bars = 75 μ m.

Table 1. Relationship Between Laminin γ 2 Expression and Clinicopathologic Characteristics in GC

	Laminin γ 2		P value
	Positive	Negative	
T classification			
T1	9 (19%)	39	.5345
T2/3/4	26 (25%)	79	
N classification			
N0	8 (12%)	60	.0037
N1/2/3	27 (32%)	58	
Stage			
I/II	15 (17%)	75	.0330
III/IV	20 (32%)	43	
Histologic classification			
Diffuse-scattered type	10 (28%)	26	.4966
Other types	25 (21%)	92	

expression in Wnt5a-positive GC cases (10 of 24 cases; 42%) was significantly higher than that in Wnt5a-negative GC cases (0 of 12 cases, 0%; $P = .0146$) (Table 2). There was a tendency for laminin γ 2 to be expressed in GC cells expressing Wnt5a (Figure 6A and B and Supplementary Figure 2). In contrast, among 117 other types of GC cases, the frequency of laminin γ 2 expression in Wnt5a-positive GC cases (5 of 20 cases; 25%) was not different from that in Wnt5a-negative GC cases (20 of 97 cases, 21%; $P = .7649$) (Table 2). However, in 5 GC cases positive for both Wnt5a and laminin γ 2, there was a tendency for GC cells stained by laminin γ 2 to also be positive for Wnt5a (Supplementary Figure 2). These results suggest that Wnt5a is involved in laminin γ 2 expression, at least in diffuse-scattered type GC.

To examine the relationship between expression of β -catenin and laminin γ 2, further immunohistochemical analysis of β -catenin was performed on 153 GC cases. Cancer cells showing cytoplasmic or nuclear accumulation of β -catenin were not always positive for laminin γ 2 (Figure 6E and F and Table 2).

Discussion

Wnt5a Induces Expression of Laminin γ 2

The results of this study showed for the first time that Wnt5a is involved in the metastasis of GC cells in vivo using nude mice. It was also found that Wnt5a induces the expression of laminin γ 2 in at least 3 different GC cell lines and that laminin γ 2 mediates Wnt5a-dependent invasion. From the results in biochemical, reporter gene, and ChIP assays, the possible mechanism by which Wnt5a induces the expression of laminin γ 2 in GC cells is that the binding of Wnt5a to Fz2 would stimulate the expression of laminin γ 2 by the recruitment of JunD to the AP-1 binding site of the promoter region of the *LAMC2* gene through the activation of PKC and JNK. Immunohistochemical studies have shown that laminin γ 2 is overexpressed at the invasive front of hu-

man cancers.^{14,15} Taken together with previous clinicopathologic studies showing that the expression of Wnt5a is associated with aggressiveness and poor prognosis in GC,⁶ these results suggest that laminin γ 2 is involved in aggressiveness of GC in which Wnt5a is highly expressed.

Although the molecular mechanism by which laminin γ 2 stimulates the migration of cancer cells is not understood, the proteolysis of laminin γ 2 to 105-kilodalton and 70-kilodalton fragments increases cell motility activity but decreases its cell adhesion activity.¹¹ In addition, it has also been reported that domain III of laminin γ 2 stimulates cell migration by binding to epidermal growth factor receptor²⁵ and that the 70-kilodalton fragment binds to syndecan-1 and disrupts the hemidesmosome-like structure.²⁶ The cleaved form of laminin γ 2 was indeed produced in the extracellular matrix fraction from MKN-45 cells overexpressing Wnt5a (see Figure 2D). Therefore, production of proteases, such as metalloproteinases, from cancer cells may cooperate to enhance the effects of laminin γ 2 on cancer cells.

β -Catenin activates laminin γ 2 gene expression through the 2 Tcf-binding elements in colorectal cancer.²² It was found that the activation of Wnt5a and β -catenin pathways induces the expression of laminin γ 2 independently in cultured GC cells. It is notable that overexpression of Tcf-4 is required for β -catenin-dependent laminin γ 2 expression in this assay. Because it was reported that Tcf-4E is expressed in colon cancer where β -catenin is up-regulated,²⁷ expression of β -catenin could induce the expression of laminin γ 2 in colon cancer. However, it is unlikely that the β -catenin pathway stimulates the

Table 2. Relationship Between Laminin γ 2 Protein Expression and Wnt5a or β -Catenin in GC

	Laminin γ 2		P value
	Positive	Negative	
All cases (n = 153)			
Wnt5a			
Positive	15 (34%)	29	.0543
Negative	20 (18%)	89	
β -catenin			
Positive	4 (18%)	18	.7847
Negative	31 (24%)	100	
Diffuse-scattered type (n = 36)			
Wnt5a			
Positive	10 (42%)	14	.0146
Negative	0 (0%)	12	
β -catenin			
Positive	0 (0%)	2	1.0000
Negative	10 (29%)	24	
Other types (n = 117)			
Wnt5a			
Positive	5 (25%)	15	.7649
Negative	20 (21%)	77	
β -catenin			
Positive	4 (20%)	16	1.0000
Negative	21 (22%)	76	

expression of laminin γ 2 in GC, because an immunohistochemical study suggested that accumulation of β -catenin in GC cases is not associated with laminin γ 2 expression. The expression level of Tcf-4 may not change in GC cells overexpressing β -catenin.

Clinical Relevance of the Coexpression of Wnt5a and Laminin γ 2 in GC

It was shown previously that Wnt5a is expressed in diffuse-scattered type (scirrhous type) GC more frequently than in other types of GC.⁶ Scirrhous GC is characterized by extensive cancer cell infiltration and proliferation accompanied by abundant stromal fibrosis, and the prognosis of patients with scirrhous GC remains poor.²⁸ One reason for the poor prognosis is rapid infiltration of cancer cells. It has been reported that abnormalities in several molecules are involved in the pathogenesis of scirrhous GC. The present study found that the coexpression of Wnt5a and laminin γ 2 in the same cancer cells is observed at a statistically significant rate in diffuse-scattered type GC but not in other GC types. Wnt5a stimulates cell migration by activating Rac and focal adhesion kinase.^{6,9} In addition to this pathway, Wnt5a induces the expression of laminin γ 2 by activating JNK (this study) and JNK also phosphorylates paxillin, resulting in stimulation of cell motility.²⁹ Therefore, the activation of these pathways by Wnt5a overexpressed in scirrhous GC may trigger invasion and metastasis by GC cells, resulting in poor prognosis. Among GC cell lines, KKLS cells barely expressed laminin γ 2, although Wnt5a was required for in vivo metastasis and in vitro invasion. These results suggest that Wnt5a also activates other pathways that are involved in invasion and metastasis.

Supplementary Data

Note: To access the supplementary material accompanying this article, visit the online version of *Gastroenterology* at www.gastrojournal.org, and at doi: 10.1053/j.gastro.2009.02.003.

References

- Ohgaki H, Matsukura N. Stomach cancer. Lyon, France: IARC Press, 2003.
- Hohenberger P, Gretschel S. Gastric cancer. *Lancet* 2003;362:305–315.
- Gupta GP, Massague J. Cancer metastasis: building a framework. *Cell* 2006;127:679–695.
- Yokozaki H. Molecular characteristics of eight gastric cancer cell lines established in Japan. *Pathol Int* 2000;50:767–777.
- Saitoh T, Mine T, Katoh M. Frequent up-regulation of WNT5A mRNA in primary gastric cancer. *Int J Mol Med* 2002;9:515–519.
- Kurayoshi M, Oue N, Yamamoto H, et al. Expression of Wnt-5a is correlated with aggressiveness of gastric cancer by stimulating cell migration and invasion. *Cancer Res* 2006;66:10439–10448.
- Weeraratna AT, Jiang Y, Hostetter G, et al. Wnt5a signaling directly affects cell motility and invasion of metastatic melanoma. *Cancer Cell* 2002;1:279–288.
- Kikuchi A, Yamamoto H. Tumor formation due to abnormalities in the β -catenin-independent pathway of Wnt signaling. *Cancer Sci* 2008;99:202–208.
- Kurayoshi M, Yamamoto H, Izumi S, et al. Post-translational palmitoylation and glycosylation of Wnt-5a are necessary for its signalling. *Biochem J* 2007;402:515–523.
- Hintermann E, Quaranta V. Epithelial cell motility on laminin-5: regulation by matrix assembly, proteolysis, integrins and erbB receptors. *Matrix Biol* 2004;23:75–85.
- Miyazaki K. Laminin-5 (laminin-332): unique biological activity and role in tumor growth and invasion. *Cancer Sci* 2006;97:91–98.
- Fukushima Y, Ohnishi T, Arita N, et al. Integrin α 3 β 1-mediated interaction with laminin-5 stimulates adhesion, migration and invasion of malignant glioma cells. *Int J Cancer* 1998;76:63–72.
- Kariya Y, Tsubota Y, Hirosaki T, et al. Differential regulation of cellular adhesion and migration by recombinant laminin-5 forms with partial deletion or mutation within the G3 domain of α 3 chain. *J Cell Biochem* 2003;88:506–520.
- Pyke C, Romer J, Kallunki P, et al. The γ 2 chain of laminin/laminin 5 is preferentially expressed in invading malignant cells in human cancers. *Am J Pathol* 1994;145:782–791.
- Koshikawa N, Moriyama K, Takamura H, et al. Overexpression of laminin γ 2 chain monomer in invading gastric carcinoma cells. *Cancer Res* 1999;59:5596–5601.
- Lauren P. The two histological main types of gastric carcinoma: diffuse and so-called intestinal-type carcinoma. An attempt at a histo-clinical classification. *Acta Pathol Microbiol* 1965;64:31–49.
- Tsuchiya Y, Sato H, Endo Y, et al. Tissue inhibitor of metalloproteinase 1 is a negative regulator of the metastatic ability of a human gastric cancer cell line, KKLS, in the chick embryo. *Cancer Res* 1993;53:1397–1402.
- Fidler IJ. Critical factors in the biology of human cancer metastasis: twenty-eighth G.H.A. Clowes Memorial Award Lecture. *Cancer Res* 1990;50:6130–6138.
- Olsen J, Lefebvre O, Fritsch C, et al. Involvement of activator protein 1 complexes in the epithelium-specific activation of the laminin γ 2-chain gene promoter by hepatocyte growth factor (scatter factor). *Biochem J* 2000;347:407–417.
- Yamanaka H, Moriguchi T, Masuyama N, et al. JNK functions in the non-canonical Wnt pathway to regulate convergent extension movements in vertebrates. *EMBO Rep* 2002;3:69–75.
- Kikuchi A, Yamamoto H, Kishida S. Multiplicity of the interactions of Wnt proteins and their receptors. *Cell Signal* 2007;19:659–671.
- Hlubek F, Jung A, Kotzner N, et al. Expression of the invasion factor laminin γ 2 in colorectal carcinomas is regulated by β -catenin. *Cancer Res* 2001;61:8089–8093.
- Mikels AJ, Nusse R. Purified Wnt5a protein activates or inhibits β -catenin-TCF signaling depending on receptor context. *PLoS Biol* 2006;4:570–582.
- Korinek V, Barker N, Morin PJ, et al. Constitutive transcriptional activation by a β -catenin-Tcf complex in APC^{-/-} colon carcinoma. *Science* 1997;275:1784–1787.
- Schenk S, Hintermann E, Bilban M, et al. Binding to EGF receptor of a laminin-5 EGF-like fragment liberated during MMP-dependent mammary gland involution. *J Cell Biol* 2003;161:197–209.
- Ogawa T, Tsubota Y, Hashimoto J, et al. The short arm of laminin γ 2 chain of laminin-5 (laminin-332) binds syndecan-1 and regulates cellular adhesion and migration by suppressing phosphorylation of integrin β 4 chain. *Mol Biol Cell* 2007;18:1621–1633.

27. Atcha FA, Munguia JE, Li TW, et al. A new β -catenin-dependent activation domain in T cell factor. *J Biol Chem* 2003;278:16169–16175.
28. Tahara E. Growth factors and oncogenes in human gastrointestinal carcinomas. *J Cancer Res Clin Oncol* 1990;116:121–131.
29. Huang C, Rajfur Z, Borchers C, et al. JNK phosphorylates paxillin and regulates cell migration. *Nature* 2003;424:219–223.

Received September 3, 2008. Accepted February 5, 2009.

Reprint requests

Address requests for reprints to: Akira Kikuchi, MD, PhD, Department of Biochemistry, Graduate School of Biomedical Sciences, Hiroshima University 1-2-3 Kasumi, Minami-ku,

Hiroshima 734-8551, Japan. e-mail: akikuchi@hiroshima-u.ac.jp; fax: (81) 82-257-5134.

Acknowledgments

The authors thank Dr K. Miyazaki (Yokohama City University) for providing anti-laminin α 3 antibody.

Conflicts of interest

The authors disclose no conflicts.

Funding

Supported by Grants-in-Aid for Scientific Research and for Scientific Research on priority areas from the Ministry of Education, Science, and Culture of Japan (2006, 2007, 2008) and by the Uehara Memorial Foundation (2007).

Characteristic gene expression in stromal cells of gastric cancers among atomic-bomb survivors

Naohide Oue¹, Kazuhiro Sentani¹, Naoya Sakamoto¹, Junichi Motoshita¹, Takashi Nishisaka², Toshiyuki Fukuhara², Hiroo Matsuura³, Hiroki Sasaki⁴, Kei Nakachi⁵ and Wataru Yasui^{1*}

¹*Department of Molecular Pathology, Hiroshima University Graduate School of Biomedical Sciences, Hiroshima, Japan*

²*Department of Pathology and Laboratory Medicine, Hiroshima Prefectural Hospital, Hiroshima, Japan*

³*Pathology, Hiroshima Citizens Hospital, Hiroshima, Japan*

⁴*Genetics Division, National Cancer Center Research Institute, Tokyo, Japan*

⁵*Department of Radiobiology/Molecular Epidemiology, Radiation Effects Research Foundation, Hiroshima, Japan*

Characteristic gene expression in stromal cells of gastric cancers among atomic-bomb survivors

Naohide Oue¹, Kazuhiro Sentani¹, Naoya Sakamoto¹, Junichi Motoshita¹, Takashi Nishisaka², Toshiyuki Fukuhara², Hiroo Matsuura³, Hiroki Sasaki⁴, Kei Nakachi⁵ and Wataru Yasui^{1*}

¹Department of Molecular Pathology, Hiroshima University Graduate School of Biomedical Sciences, Hiroshima, Japan

²Department of Pathology and Laboratory Medicine, Hiroshima Prefectural Hospital, Hiroshima, Japan

³Pathology, Hiroshima Citizens Hospital, Hiroshima, Japan

⁴Genetics Division, National Cancer Center Research Institute, Tokyo, Japan

⁵Department of Radiobiology/Molecular Epidemiology, Radiation Effects Research Foundation, Hiroshima, Japan

To elucidate the mechanism of radiation-induced cancers, molecular analysis of cancers in atomic-bomb survivors is important. In our study, we developed a custom oligonucleotide array of 208 genes. We analyzed gene expression profiles of gastric cancers (GCs) from atomic-bomb survivors and identified 9 genes with significantly lower expression in GCs from exposed patients than in GCs from nonexposed patients. Among these 9 genes, expression of versican and osteonectin was investigated in greater detail using immunohistochemistry in 116 GCs from 64 exposed and 52 nonexposed patients who developed GC after the bombing. In the Stage I/II GCs, the clinicopathologic, phenotypic and proliferative characteristics of GCs from exposed and nonexposed patients did not differ significantly; however, versican and osteonectin were expressed at much lower levels in the area of tumor-associated stroma of exposed patients than in nonexposed patients ($p = 0.026$ and $p = 0.024$, respectively). These results suggest that the characteristics of tumor-associated stromal cells differ between GCs from exposed and nonexposed patients.

© 2008 Wiley-Liss, Inc.

Key words: gastric cancer; radiation carcinogenesis; atomic bomb; versican; osteonectin

More than 60 years have passed since atomic-bomb (A-bomb) exposure in Hiroshima and Nagasaki. A prospective cohort study [Life Span Study (LSS)] of 120,000 subjects has been conducted by the Radiation Effects Research Foundation (RERF).¹ Solid cancers, including breast, colon, lung and stomach, have a long latency period, and the excess relative risks of solid cancers remain high, specifically among those exposed when young.¹ Although approximately half of the LSS members have already deceased, cancer mortality in the LSS has continued to increase with the aging of this population, and it is anticipated to peak in 2015. Previous studies conducted to elucidate the mechanism of radiation-associated carcinogenesis mainly used formalin-fixed and paraffin-embedded archival tissues,^{2,3} which are not suitable for selected molecular analyses (e.g. quantitative assays of gene expression) because of degradation of RNA.

According to the World Health Organization, gastric cancer (GC) is the fourth most common malignancy world wide, with ~870,000 new cases occurring yearly. Cancer develops as a result of multiple genetic and epigenetic alterations.^{4,5} Better knowledge of changes in gene expression that occur during gastric carcinogenesis may lead to improvements in diagnosis, treatment and prevention of GC. Thus far, the effect of radiation on GC development has been estimated on the basis of the LSS, in which both mortality and incidence were used as end points. The excess relative risks per gray (Gy) were 1.20 for mortality⁶ and 1.32 for incidence.¹ Although several genetic alterations, including mutations in *TP53* and *BRAF*, have been reported in selected cancers of A-bomb survivors,^{2,3,7} changes in gene expression have not been investigated. Furthermore, specific mutations for radiation-associated cancers have not been reported.

In our study, we performed custom array analysis of GCs from A-bomb survivors. We found reduced expression of versican and osteonectin in GCs from exposed patients. Versican, a large chon-

droitin sulfate proteoglycan, belongs to the aggrecan gene family.⁸ Versican is a component of the extracellular matrix (ECM) of various soft tissues and is involved in a number of pathologic processes including cancer, atherosclerotic vascular diseases and so on.⁹ Versican represses cell adhesion and promotes proliferation, migration, and invasion.^{10,11} Increased stromal versican deposition correlates with breast cancer relapse and prostate cancer progression.^{12,13} Osteonectin, a matricellular glycoprotein, modulates the interaction of cells with the ECM through its regulation of cell adhesion and matrix assembly.¹⁴ Increased expression of osteonectin has been reported in several human cancers, and stromal osteonectin expression has been shown to correlate with tumor progression and poor survival.^{15,16} Osteonectin enhances the invasive capacity of prostate and breast cancer cells.^{17,18} Although overexpression of versican and osteonectin has been reported in GC,^{19,20} the relationship with radiation exposure history of patients has not been studied. Therefore, we performed immunohistochemical analysis of versican and osteonectin expression in 116 GCs from A-bomb survivors.

Material and methods

Tissue samples

Primary tumor samples from 136 patients with GC were collected. Patients were treated at Hiroshima University Hospital (Hiroshima, Japan) or at an affiliated hospital. All patients underwent curative resection. Only patients who did not undergo preoperative radio- or chemotherapy and did not have clinical evidence of distant metastasis were enrolled in the study.

For use in our oligonucleotide array analysis, 3 freshly frozen GC tissue samples from exposed patients (5, 7 and 18 mGy) were obtained during surgery at the Department of Surgical Oncology, Hiroshima University Hospital, between 2004 and 2005. These patients were A-bomb survivors (3 LSS cohort members, RERF) in Hiroshima, Japan, who developed GC after the bombing. Their corresponding nonneoplastic mucosa samples were also available. In addition, we analyzed 20 freshly frozen GC tissue samples from nonexposed patients, who underwent surgery between 1991 and 1998 at the Department of Surgical Oncology, Hiroshima University Hospital; they were neither A-bomb survivors nor the LSS cohort members. Of these 20 GC samples, 10 corresponding nonneoplastic mucosa samples were available. All 20 GC samples were obtained during surgery at Hiroshima University Hospital.

Grant sponsors: Ministry of Education, Culture, Science, Sports, and Technology of Japan; Ministry of Health, Labour and Welfare of Japan.

*Correspondence to: Department of Molecular Pathology, Hiroshima University Graduate School of Biomedical Sciences, 1-2-3 Kasumi, Minami-ku, Hiroshima 734-8551, Japan. Fax: +81-82-257-5149.

E-mail: wyasui@hiroshima-u.ac.jp

Received 18 January 2008; Accepted after revision 29 September 2008

DOI 10.1002/ijc.24060

Published online 9 October 2008 in Wiley InterScience (www.interscience.wiley.com).

We confirmed microscopically that the tumor specimens were predominantly (>50%, on a nuclear basis) cancer tissue. Samples were frozen immediately in liquid nitrogen and stored at -80°C until use.

For immunohistochemical analysis, we used formalin-fixed and paraffin-embedded archival tissues from 116 patients with GC who underwent surgery between 1975 and 2005 at the Department of Surgical Oncology, Hiroshima University Hospital. All 116 patients were A-bomb survivors (LSS cohort members) in Hiroshima, Japan. Although these patients were survivors who developed GC after the bombing, they were further classified according to the levels of exposed radiation dose (*i.e.* ≥ 5 mGy and < 5 mGy were defined as "exposed" and "nonexposed," respectively): 64 exposed (median dose, 51 mGy) and 52 nonexposed patients.

Tumor staging was performed according to the TNM classification system.²¹ Histologic classification of GC was carried out according to the Lauren classification system.²² The detailed procedures for acquiring informed consent from study patients and collecting tissue specimens were as described previously.²³ In accordance with the Ethical Guidelines for Human Genome/Gene Research enacted by the Japanese Government, tissue specimens were collected and used on the basis of the approval from the Ethical Review Committee of the Hiroshima University School of Medicine and from the ethical review committees of collaborating organizations.

Radiation dose

A-bomb radiation doses were estimated with the DS02 system.²⁴

Oligonucleotide array construction

Probes, which were all 65 bp in length, were designed to have approximately the same annealing temperature. The oligonucleotide array, GenopalTM (Mitsubishi Rayon, Tokyo, Japan), was made as described previously.²⁵ In brief, plastic hollow fibers were bundled in an orderly arrangement and hardened with resin to form a block. Oligonucleotide-capture probes were chemically bonded inside each hollow fiber with hydrophilic gel. The block was then sliced into thin chips, each of which was set in a holder (www.mrc.co.jp/genome/about/process.html for details). The array contained 208 genes, including GC-related genes identified by our previous SAGE analysis,²⁶ known genes related to development and progression of GC,^{27,28} genes related to DNA damage response and repair and genes associated with sensitivity to anti-cancer drugs.²⁹ A list of the genes on the array is available upon request.

Preparation of labeled probe, hybridization, detection and data analysis

Total RNA was isolated from frozen tissue with Isogene (Nippon Gene, Tokyo, Japan), according to the manufacturer's protocol. Quantification and integrity of RNA were assessed with an Agilent 2100 Bioanalyzer and RNA 6000 LabChip Kit (Agilent Technologies, Palo Alto, CA). One microgram of total RNA was used to prepare antisense biotinylated RNA with MessageAmpTM II-Biotin Enhanced Single Round aRNA Amplification Kit (Ambion, Austin, TX) per the manufacturer's instructions. The biotinylated cRNAs were then cleaned up and fragmented. Hybridization was carried out with the oligonucleotide array in 100 μl of hybridization buffer (0.12 M Tris HCl/0.12 M NaCl/0.05% Tween-20 and 5 μg of fragmented biotinylated aRNA) at 65°C overnight. After hybridization, the oligonucleotide arrays were washed twice in 0.12 M Tris HCl/0.12 M NaCl/0.05% Tween-20 at 65°C for 20 min, followed by washing in 0.12 M Tris HCl/0.12 M NaCl for 10 min, before being cooled slowly to room temperature. After staining with streptavidin-Alexa Fluor 647 (Invitrogen, Carlsbad, CA), the Genopal array was scanned, and the image was captured with a cooled CCD-type Microarray Image Analyzer (Mitsubishi Rayon). Fluorescence intensity was analyzed with

software developed by Mitsubishi Rayon. Fluorescence throughout the 3-dimensional structure of each array feature can be efficiently captured because of the long focal depth of the optical system of the image analyzer (www.mrc.co.jp/genome/about/analysis.html). After image acquisition and quantification, spots with signal intensity lower than or equal to that of the background were identified and excluded from the analysis. Next, background-subtracted spot intensities were normalized so that the *ACTB* gene signal would be 10,000.

Immunohistochemistry

Formalin-fixed and paraffin-embedded samples were sectioned, deparaffinized and stained with H&E to ensure that the sectioned block contained tumor cells. Adjacent sections were then stained immunohistochemically with a Dako Envision + Rabbit Peroxidase Detection System (Dako Cytomation, Carpinteria, CA) or Dako Envision + Mouse Peroxidase Detection System (Dako Cytomation). Antigen retrieval was done by microwave heating in citrate buffer (pH 6.0) for 30 min. After peroxidase activity was blocked with 3% H_2O_2 -methanol for 10 min, sections were incubated with normal goat serum (Dako Cytomation) for 20 min to block nonspecific antibody binding sites. Sections were incubated with primary antibodies against transketolase (dilution 1:50; Santa Cruz Biotechnology, Santa Cruz, CA), versican (1:50; Seikagaku Corporation, Tokyo, Japan), THBS-2 (1:50; Santa Cruz Biotechnology), PDGF receptor- β (1:50; Santa Cruz Biotechnology), ribonuclease A (1:50; Abcam, Cambridge, UK), osteonectin (1:50; Novocastra, Newcastle, UK), vimentin (1:50; Dako Cytomation) and Ki67 (1:50; Dako Cytomation) for 1 hr at room temperature, followed by incubations with Envision + antirabbit peroxidase or Envision + antimouse peroxidase for 30 min each. Staining was completed with 10 min incubation with the substrate-chromogen solution. Sections were counterstained with 0.1% hematoxylin. For the Ki67-index, 1,000 nuclei were counted to evaluate the percentage of positive nuclei. The Ki67-index was considered to reflect the proliferative index.

Phenotype analysis of GC

GCs were classified into 4 phenotypes: gastric (G) type, intestinal (I) type, gastric and intestinal mixed (GI) type and unclassified (N) type. For phenotypic expression analysis of GC, we performed immunohistochemical analysis (as described earlier) with 4 antibodies: anti-MUC5AC (Novocastra) as a marker of gastric foveolar epithelial cells, anti-MUC6 (Novocastra) as a marker of pyloric gland cells, anti-MUC2 (Novocastra) as a marker of goblet cells in the small intestine and colorectum, and anti-CD10 (Novocastra) as a marker of microvilli of absorptive cells in the small intestine and colorectum. The criteria³⁰ for the classification of G-type and I-type GCs were as follows. GCs in which more than 10% of cells in the section expressed at least 1 gastric epithelial cell marker (MUC5AC or MUC6) or intestinal epithelial cell marker (MUC2 or CD10) were classified as G-type or I-type cancers, respectively. Sections that showed both gastric and intestinal phenotypes were classified as GI type, and those that lacked both the gastric and intestinal phenotypes were classified as N type.

Statistical methods

Correlation between the gene expression profiles from different sample conditions was assessed by Spearman's rank correlation coefficients. Differences in mRNA expression levels between 2 samples were tested by Mann-Whitney *U* test for individual genes. Univariate analysis for clinicopathologic, phenotypic and proliferative variables in relation to radiation exposure status was done by Mann-Whitney *U* test for continuous variables and Fisher's exact test for categorical variables. Associations between clinicopathologic variables and immunostaining for versican or osteonectin were analyzed by Fisher's exact test. Multivariate logistic regression analysis was carried out to assess the relationship among clinicopathologic characteristics, expression of versican

and osteonectin, and radiation exposure status. A p value of <0.05 was considered statistically significant.

Results

Custom array analysis

Toward identification of potential molecular markers for radiation-associated cancer and also better understanding of its molecular mechanisms, we designed a custom oligonucleotide array comprising 208 genes (Fig. 1). Because this platform has not been characterized, we first validated the performance of this array before analyzing the GCs from exposed patients. To validate the array, total RNA was isolated from the MKN-1 cell line. RNA quality was assessed with a Bioanalyzer (Agilent), and the RNA integrity number (RIN) was confirmed to be 10.0. The isolated RNA was divided into 5 tubes (Samples 1–5), and we subjected the RNA in each tube to a different preparation condition. To analyze the effect of the amount of total RNA, we prepared 3 samples. Sample 1 contained 1.0 μg total RNA, Sample 2 contained 2.0 μg total RNA and Sample 3 contained 0.5 μg total RNA. To analyze the effect of RNA quality, we prepared 2 RNA samples with different RINs. Sample 4 was frozen and thawed 20 times, and Sample 5 was frozen and thawed 40 times. The RNA quality was then assessed with the Bioanalyzer. The RIN of Sample 4 was 8.2 and that of Sample 5 was 5.9. Probes derived from these 5 samples were hybridized simultaneously (Fig. 1). Although the condition of each sample differed, gene expression levels from Sample 1 obtained by oligonucleotide array correlated well with those from Sample 2 ($p < 0.0001$, $r = 0.95$), Sample 3 ($p < 0.0001$, $r = 0.96$), Sample 4 ($p < 0.0001$, $r = 0.98$) and Sample 5 ($p < 0.0001$, $r = 0.97$) (Fig. 1). Therefore, 1 μg of total RNA (RIN > 6.0) was used for further array analysis.

We next analyzed the gene expression profiles of GCs from exposed and nonexposed patients by custom oligonucleotide array. Freshly frozen GC tissue samples were obtained from 3 exposed patients (Cases EX01, EX02 and EX03, with radiation dose 7, 5 and 18 mGy, respectively) as well as their corresponding nonneoplastic mucosa samples. Clinicopathologic features of these exposed patients are shown in Table I. Histologically, EX01 was intestinal-type GC of Lauren classification, EX02 was diffuse-type GC of Lauren classification, and EX03 was an α -fetoprotein (AFP)-producing hepatoid adenocarcinoma (Fig. 2a). Immunostaining of EX03 revealed that AFP was present in cancer cells (Fig. 2a). On the other hand, when we analyzed 20 freshly frozen GC tissues from nonexposed patients (Cases NEX01 to NEX20), unsupervised clustering showed that the exposed and nonexposed patients could not be distinguished on the basis of mRNA expression (data not shown). To determine whether there is a gene expression profile characteristic to exposed patients, we compared expression levels of individual genes between exposed and nonexposed patients. Finally, we found 9 genes whose expression was significantly lower in GC from exposed patients than in GC from nonexposed patients (Table II). No gene showed higher expression in GC from exposed patients than in GC from nonexposed patients.

Among these 9 genes, antibodies against proteins encoded by *TKT* (encoding transketolase), *VCAN* (encoding versican), *THBS2* (encoding THBS-2), *PDGFRB* (encoding PDGF receptor- β), *RNASE1* (encoding ribonuclease A) and *SPARC* (encoding osteonectin) were commercially available. We performed immunohistochemistry of these 6 molecules in 3 formalin-fixed and paraffin-embedded archival GC tissue samples from exposed patients and 10 GC samples from nonexposed patients analyzed by oligonucleotide array to compare oligonucleotide array data and immunostaining results. The immunostaining results for versican (encoded by *VCAN*) and osteonectin (encoded by *SPARC*) were consistent with those of the oligonucleotide array. It has been reported that immunoreactivity for versican was present in tumor-stroma associated with malignant areas and in blood vessel walls.³¹ In Case EX03 (exposed patient), expression of versican (*VCAN*) mRNA

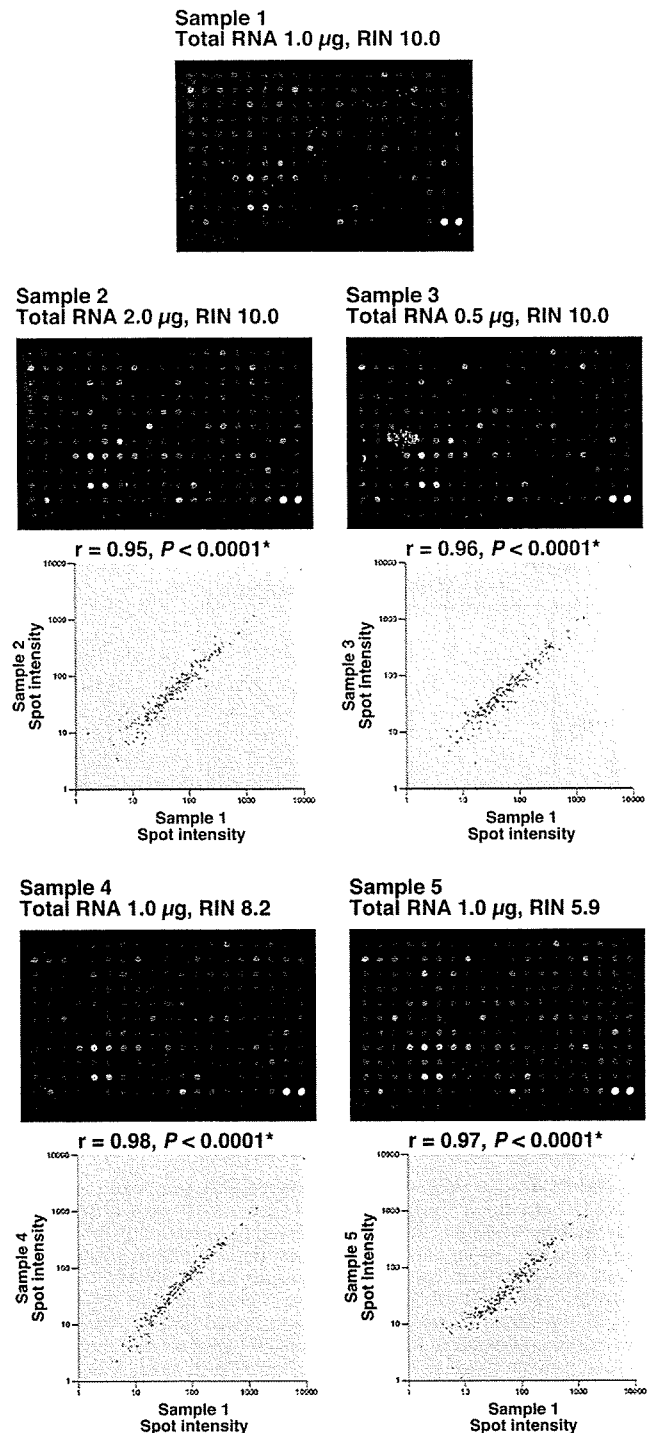


FIGURE 1 – Custom oligonucleotide array analysis of GCs from exposed and nonexposed patients. Images of hybridization results for probes prepared under 5 different conditions. The oligonucleotide arrays' intensity data for Samples 1 and 2, Samples 1 and 3, Samples 1 and 4 and Samples 1 and 5 are plotted against each other. *Spearman's rank correlation coefficient.

on the oligonucleotide array was low, and immunohistochemistry revealed that tumor-associated stroma did not express versican despite staining of versican in blood vessel walls (Fig. 2b). In Case EX01 and Case EX02, versican staining was not observed. In Case NEX03 (nonexposed patient), strong and extensive staining

TABLE I – CLINICOPATHOLOGIC CHARACTERISTICS OF THE 3 GASTRIC CANCERS FROM EXPOSED PATIENTS ANALYZED BY OLIGONUCLEOTIDE ARRAY

Sample name	Age (years)	Sex	T grade	N grade	M grade	Stage	Histologic classification	Radiation dose (mGy)
EX01	72	Female	2	0	0	I	Intestinal	7
EX02	75	Male	2	1	0	II	Diffuse	5
EX03	62	Female	2	1	0	II	Hepatoid	18

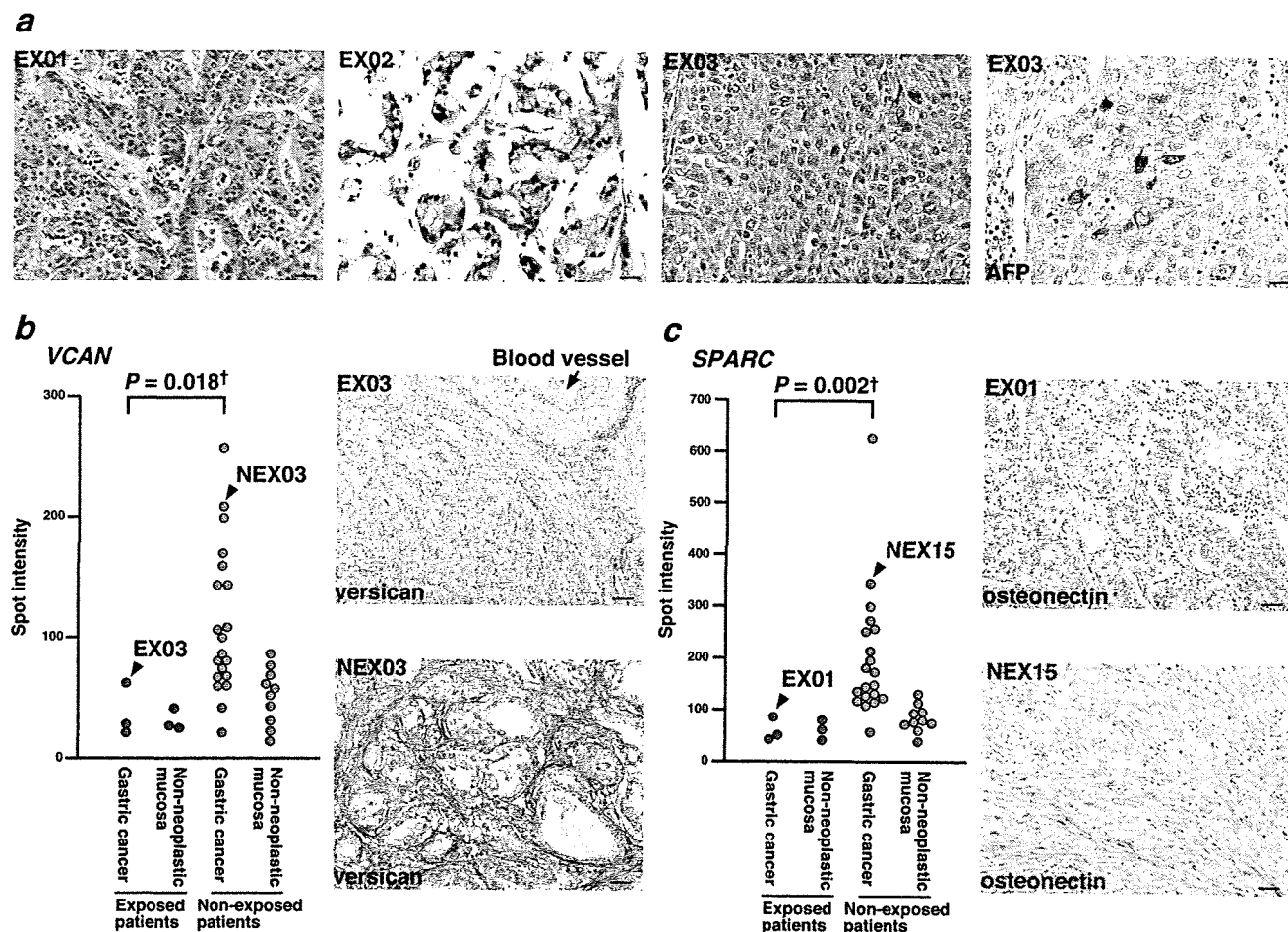


FIGURE 2 – (a) H&E-stained sections of GCs from exposed patients analyzed by custom oligonucleotide array. Case EX01 was an intestinal-type GC of Lauren classification, and Case EX02 was a diffuse-type GC of Lauren classification. EX03 was an AFP-producing hepatoid adenocarcinoma. Staining of AFP was observed in tumor cells (brown color). Bar: 25 μ m. (b) Analyses of expression of *VCAN* mRNA (which encodes versican) by custom oligonucleotide array (left) and expression of versican protein by immunohistochemistry (right) in GCs from exposed and nonexposed patients. Each point represents the *VCAN* mRNA expression level. †Mann–Whitney *U* test. Immunostaining of versican in GC from exposed patients (Case EX03) and nonexposed patients (Case NEX03) revealed that tumor-associated stromal cells express versican. Versican staining in blood vessel wall was also observed (arrow). Bar: 50 μ m. (c) Analyses of expression of *SPARC* mRNA (which encodes osteonectin) by custom oligonucleotide array (left) and expression of osteonectin protein by immunohistochemistry (right) in GCs from exposed and nonexposed patients. Each point represents the *SPARC* mRNA expression level. †Mann–Whitney *U* test. In GC from exposed patients (Case EX01) and nonexposed patients (Case NEX15), tumor-associated stromal cells express osteonectin. Bar: 50 μ m.

of versican was observed in tumor-associated stroma (Fig. 2b). Stromal versican staining was also found in several GC cases from nonexposed patients. In addition to versican, osteonectin has also been reported to be stained in tumor-associated stroma. In Case EX01 (exposed patient), expression of osteonectin (*SPARC*) mRNA on the oligonucleotide array was low, and a small fraction of tumor-associated stromal cells was shown to express osteonectin by immunohistochemistry (Fig. 2c). In Case EX02 and Case EX03, osteonectin staining was not observed. In contrast, in Case NEX15 (nonexposed patient), extensive staining of osteonectin was observed in tumor-associated stroma (Fig. 2c). Stromal osteonectin staining was also found in several GC cases from nonexposed patients. Immunostaining of the remaining 4 molecules

(transketolase, THBS-2, PDGF receptor- β and ribonuclease A) did not differ significantly between exposed and nonexposed patients. Therefore, we decided to perform immunostaining of versican and osteonectin in additional GC cases.

Clinicopathologic features, mucin phenotypes and proliferative characteristics of survivor patients

To validate the reduced expression of versican and osteonectin in GC from exposed patients, we collected formalin-fixed and paraffin-embedded archival tissues from 116 patients with GC who underwent surgical resection. All 116 patients were A-bomb survivors (LSS cohort members) in Hiroshima, Japan, and comprised

64 exposed (median dose, 51 mGy; range, 5–2,601 mGy) and 52 nonexposed patients (range, 0–4 mGy) who developed GC after the bombing. Patient characteristics such as latency period (years elapsed from A-bombing to diagnosis, defined only for exposed patients), age at the time of A-bombing, histologic type, sex, age at diagnosis, T grade, N grade and tumor stage are summarized in Table III. Clinicopathologic characteristics of patients did not statistically differ between exposed and nonexposed patients. Diffuse-type GC was found more frequently in exposed patients than in nonexposed patients, but the difference was not statistically significant ($p = 0.085$).

Despite the usefulness of the Lauren classification, it was previously reported that GC can be subdivided according to mucin expression into 4 phenotypes (G type, I type, GI type and N type).³² Several distinct genetic and epigenetic changes have been reported to be associated with G-type and I-type GCs.^{33–35} Therefore, we investigated the mucin phenotypes of 116 GCs: Gastric

(MUC5AC and MUC6) and intestinal (MUC2 and CD10). MUC5AC was detected in 57 of 116 (49%) cases, MUC6 in 37 (32%) cases, MUC2 in 34 (29%) cases and CD10 in 25 (22%) cases. Expression of these 4 markers did not differ statistically between exposed and nonexposed patients (data not shown). In addition, distribution of the G, I, GI and N phenotypes did not differ significantly between exposed and nonexposed patients (data not shown).

Phenotypic shift from G-type to I-type GC along with tumor progression has been reported.³² Therefore, mucin phenotypes and immunostaining of MUC5AC, MUC6, MUC2 and CD10 were analyzed with respect to tumor stages. In Stage I/II, expression of the 4 markers did not differ significantly between exposed and nonexposed patients (data not shown). In contrast, in Stage III/IV, some GCs from exposed patients showed extensive staining of MUC6 (Fig. 3a). In addition, staining of MUC2 was rare in GCs from exposed patients (Fig. 3a). Of 28 Stage III/IV GCs from exposed patients, MUC6 was expressed in 12 GCs (43%), whereas MUC6 was expressed in 2 (12%) of 17 Stage III/IV GCs from nonexposed patients ($p = 0.046$). In Stage III/IV cases, the frequency of MUC2 expression in GCs from exposed patients (3/28, 11%) was significantly lower than that in GCs from nonexposed patients (8/17, 47%, $p = 0.011$). There was no correlation between exposure status and MUC5AC or CD10 (data not shown). Mucin phenotypes with respect to tumor stage are shown in Figure 3b. For Stage I/II GCs, distribution of the G, I, GI and N types did not differ significantly between exposed and nonexposed patients. Among GCs from nonexposed patients, frequency of the G type slightly decreased with advancing tumor stage. In contrast, among GCs from exposed patients, frequency of the G type increased with advancing tumor stage; furthermore, frequency of the I type decreased with advancing tumor stage. However, statistical analysis showed that neither frequency of the G type (Table IV) nor I type (Table V) differed between exposed and nonexposed patients.

Proliferative characteristics of GCs from exposed and nonexposed patients were also investigated. The Ki67-index did not differ significantly between exposed and nonexposed patients (Table III). This was also the case in Stage I/II (data not shown). These results indicate that no significant differences in clinicopathologic, phenotypic and proliferative characteristics of GCs were found between exposed and nonexposed patients, at least in Stage I/II GCs.

TABLE II – NINE GENES WITH LOWER EXPRESSION IN GASTRIC CANCERS FROM EXPOSED PATIENTS THAN IN GASTRIC CANCERS FROM NONEXPOSED PATIENTS

Gene symbol	Exposure status	mRNA expression: median (range)	<i>p</i> value ¹
SPARC	Exposed	46 (39–84)	0.002
	Nonexposed	153 (55–624)	
ABCC1	Exposed	19 (15–22)	0.002
	Nonexposed	43.5 (19–101)	
RNASE1	Exposed	75 (74–100)	0.012
	Nonexposed	425 (46–1632)	
VCAN	Exposed	29 (24–63)	0.018
	Nonexposed	92 (22–258)	
THBS2	Exposed	35 (19–81)	0.018
	Nonexposed	155.5 (39–411)	
PDGFRB	Exposed	20 (18–29)	0.018
	Nonexposed	49.5 (13–138)	
TNFRSF14	Exposed	27 (25–42)	0.035
	Nonexposed	49 (29–90)	
TKT	Exposed	58 (35–100)	0.035
	Nonexposed	128 (53–253)	
FBP1	Exposed	105 (36–114)	0.046
	Nonexposed	196.5 (55–509)	

¹Mann–Whitney *U* test.

TABLE III – CLINICOPATHOLOGIC CHARACTERISTICS OF PATIENTS BY RADIATION EXPOSURE STATUS

Variable	Exposed patients (<i>n</i> = 64)	Nonexposed patients (<i>n</i> = 52)	<i>p</i> value
Median radiation dose (mGy, range)	51 (5–2601)	0 (0–4)	
Median latency period (years, range)	47 (30–60)	46 (30–57)	0.5 ¹
Median age at the time of atomic-bombing (years, range)	25 (2–47)	28 (2–47)	0.098 ¹
Sex			
Male	34	27	1.0 ²
Female	30	25	
Age at diagnosis (years)			
≤65	18	12	0.7 ²
>65	46	40	
T grade			
T1/T2	43	35	1.0 ²
T3/T4	21	17	
N grade			
N0	24	28	0.093 ²
N1/N2/N3	40	24	
Stage			
I/II	36	35	0.3 ²
III/IV	28	17	
Lauren classification			
Intestinal	35	37	0.085 ²
Diffuse	29	15	
Median Ki67-index (% , range)	33 (11–69)	39 (10–64)	0.196 ¹

¹Mann–Whitney *U* test. ²Fisher's exact test.

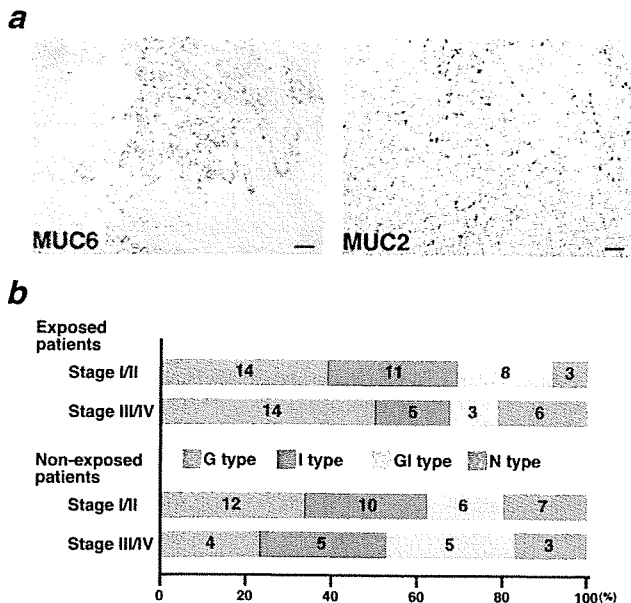


FIGURE 3 – Phenotypic analysis of GCs from exposed and nonexposed patients. (a) Immunostaining of MUC6 (exposed patient) and MUC2 (nonexposed patient). Bar: MUC6, 250 μ m; MUC2, 100 μ m. (b) Distribution of G, I, GI and N-type GCs from exposed and nonexposed patients. Numbers indicate the number of cases.

TABLE IV – SUMMARY OF THE FREQUENCY OF G-TYPE GASTRIC CANCERS IN STAGE III/IV FROM EXPOSED AND NONEXPOSED PATIENTS

	G type	Other type	p value ¹
Exposed patients	14 (50%)	14	0.118
Nonexposed patients	4 (24%)	13	

¹Fisher's exact test.

Decreased expression of versican and osteonectin in exposed patients

We performed immunostaining of versican and osteonectin in 116 GCs. In nonneoplastic gastric mucosa, although epithelial cells and stromal cells exhibited weak or no expression of versican (Figs. 4a and 4b), versican staining was observed in the walls of blood vessels (Fig. 4c). In GC tissue, tumor cells were not stained; however, versican was expressed in tumor-associated stroma. Intracellular staining of versican was detected in fibroblastic cells, because of their morphology and vimentin (a marker of fibroblasts) positivity on serial sections. Staining in fibrous bands within the tumor was also observed. The level of versican immunoreactivity was evaluated in the area of tumor-associated stroma (fibroblastic cell plus ECM). The percentage of versican-stained area of tumor-associated stroma was a continuum from 0 to 80%, and characteristic staining pattern was not observed. To analyze the relationship of versican staining to clinicopathologic characteristics, the GC cases were divided into two groups: diffuse positive group and focal positive or negative group. To maximize the statistical detection power, it is ideal that the number of diffuse positive cases/focal positive or negative cases ratio is less than 2 in nonexposed patients. When we chose 50% (50% of the area of tumor-associated stroma) as a cutoff for diffuse positive group and focal positive or negative group, 32 (62%) were diffuse positive for versican in 52 GC cases from nonexposed patients. Therefore, the immunostaining was considered diffuse positive for versican when more than 50% of the area of tumor-associated stroma was stained by versican. Of 116 GC cases, 55 (47%) were diffuse posi-

TABLE V – SUMMARY OF THE FREQUENCY OF I-TYPE GASTRIC CANCERS IN STAGE III/IV FROM EXPOSED AND NONEXPOSED PATIENTS

	I type	Other type	p value ¹
Exposed patients	5 (18%)	23	0.5
Nonexposed patients	5 (29%)	12	

¹Fisher's exact test.

tive for versican. Figure 4d illustrates the typically diffuse positive immunostaining of versican. In diffuse-type GC, strong and extensive stromal versican staining was frequently observed (Fig. 4d). Staining in fibrous bands within the tumor was also observed. Figure 4e illustrates the typically focal positive immunostaining of versican. In many GCs from exposed patients, although blood vessel wall expressed versican, staining of versican was weak or absent in stromal fibroblasts and stromal matrix (Fig. 4e). Diffuse positive GCs correlated to advanced T grade ($p = 0.003$), N grade ($p = 0.016$) and tumor stage ($p = 0.001$) (Table VI). Diffuse positive GCs were more frequently found in diffuse-type GCs than in intestinal-type GCs ($p = 0.008$) (Table 6). Focal positive or negative GCs were more frequently found in exposed patients than in nonexposed patients ($p = 0.009$) (Table 6). Because expression of versican correlated with tumor stage, versican immunostaining was analyzed by tumor stages. As shown in Table 6, in both Stage I/II and Stage III/IV GCs, focal positive or negative GCs were more frequently found in exposed patients than in nonexposed patients ($p = 0.026$ and $p = 0.023$, respectively). We then examined whether versican staining in GC from exposed patients was related to radiation dose, latency period or age at the time of A-bombing; however, there was no correlation between versican staining and any of these variables. Although versican staining was correlated with tumor stage in 116 GC cases ($p = 0.001$), multivariate logistic regression analysis revealed that expression of versican was not significant independent marker for tumor stage in 64 exposed patients ($p = 0.6$). Among 52 nonexposed patients, multivariate logistic regression analysis showed that expression of versican was not significant independent marker for tumor stage ($p = 0.9$).

We next investigated expression of osteonectin. In nonneoplastic mucosa, epithelial cells did not express osteonectin. However, in some cases, stromal cells exhibited osteonectin immunoreactivity (Fig. 4f). In GC tissues, osteonectin was stained in tumor-associated stroma; however, tumor cells were not stained. Intracellular staining of osteonectin was detected in fibroblastic cells because of their morphology and vimentin positivity on serial sections. As in a previous study,²⁰ immunoreactivity was also evident in the stromal matrix. Therefore, the levels of osteonectin immunoreactivity were evaluated in the area of tumor-associated stroma (fibroblastic cell plus ECM). The percentage of osteonectin-stained area of tumor-associated stroma ranged from 0 to 80%. Among 116 GCs, osteonectin-positive stromal cells were observed at the superficial parts of tumors in 44 (38%) cases (Fig. 4g). Osteonectin staining at the superficial parts of tumors was not correlated with T grade, N grade, tumor stage, histological type or exposure status (data not shown). To further analyze the relationship of osteonectin staining to clinicopathologic characteristics, the GC cases were divided into 2 groups: diffuse positive group and focal positive or negative group. When the same cutoff point for osteonectin and versican immunostaining was set (50% of the area of tumor-associated stroma), 20 (38%) were diffuse positive for osteonectin in 52 GC cases from nonexposed patients, and the number of diffuse positive cases/focal positive or negative cases ratio was less than 2 in nonexposed patients. Of 116 GC cases, 29 (25%) were diffuse positive for osteonectin. Figure 4h illustrates the typically diffuse positive immunostaining of osteonectin. Extensive staining of stromal cells was frequently observed in late-stage GC. Immunoreactivity was also evident in the stromal matrix. Figure 4i illustrates the typically focal positive or negative immunostaining of osteonectin. In many GCs from exposed patients, only few stromal

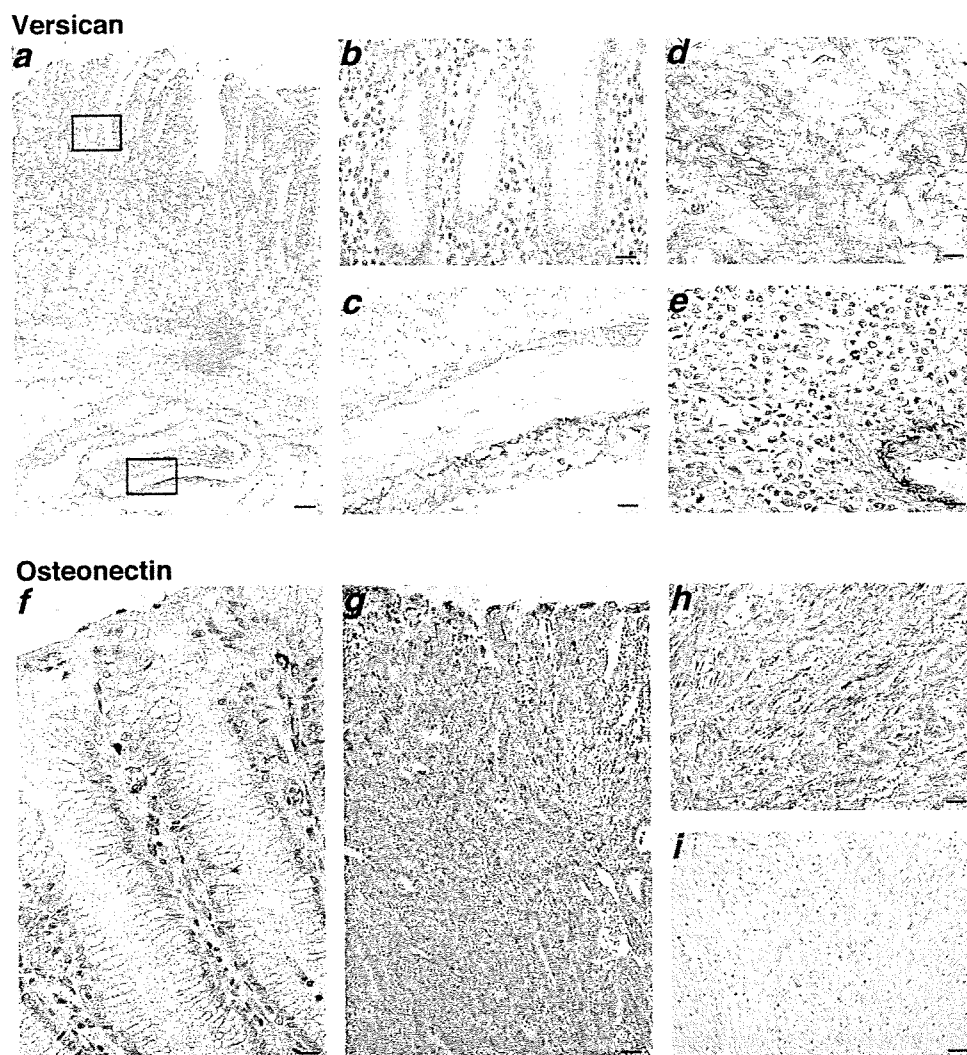


FIGURE 4 – (a–e) Immunohistochemical analysis of versican and osteonectin in 116 GCs from exposed and nonexposed patients. (a) Immunostaining of versican in GCs from exposed and nonexposed patients. (a) Nonneoplastic gastric mucosa. Panels (b) and (c) show high-magnification images of the fields indicated by boxes in panel (a). Bar: 150 μ m. (b) Foveolar epithelium in nonneoplastic gastric mucosa is negative for versican. Bar: 25 μ m. (c) Blood vessel wall in nonneoplastic gastric mucosa expresses versican. Bar: 25 μ m. (d) Stromal cells in GC from nonexposed patients express versican. Bar: 25 μ m. (e) Staining of versican was weak or absent in GCs from exposed patients. Bar: 25 μ m. (f–i) Immunostaining of osteonectin in GCs from exposed and nonexposed patients. (f) Nonneoplastic gastric mucosa. Some stromal cells are positive for osteonectin. Bar: 12 μ m. (g) In some GC cases, osteonectin-positive stromal cells are observed at the superficial part of the tumor tissue. Bar: 50 μ m. (h) Stromal cells in GC from nonexposed patients are positive for osteonectin. Bar: 50 μ m. (i) Few stromal cells are stained in GC from exposed patients. Bar: 50 μ m.

cells exhibited osteonectin staining. Immunoreactivity was not found in the stromal matrix. Diffuse positive GCs correlated to advanced T grade ($p = 0.006$), N grade ($p = 0.011$) and tumor stage ($p = 0.004$) (Table VI). Focal positive or negative GCs were more frequently found in exposed patients than in nonexposed patients ($p = 0.005$) (Table VI). Because expression of osteonectin correlated with tumor stage, we analyzed osteonectin immunostaining by tumor stage. As shown in Table VI, in both Stage I/II and Stage III/IV GCs, focal positive or negative GCs were more frequently found in exposed patients than in nonexposed patients ($p = 0.024$ and $p = 0.013$, respectively). We then examined whether osteonectin staining in GCs from exposed patients was related to radiation dose, latency period or age at the time of A-bombing; however, there was no correlation between osteonectin staining and these variables. Although diffuse positive GCs correlated to tumor stage ($p = 0.004$), multivariate logistic regression analysis revealed that expression of osteonectin was not significant independent marker for tumor stage in 64 exposed patients ($p =$

0.057). Among 52 nonexposed patients, multivariate logistic regression analysis showed that expression of osteonectin was not significant independent marker for tumor stage ($p = 0.9$).

Because clinicopathologic characteristics and expression of versican and osteonectin may be interrelated, we performed multivariate logistic analysis to determine which variables are independent markers for radiation exposure status. As shown in Table VII, multivariate logistic regression analysis revealed that both expression of versican ($p = 0.002$) and osteonectin ($p = 0.001$) were significant independent markers for GCs from exposed patients.

Discussion

Our study entails 2-stage strategy to find molecular markers that are specifically involved in radiation-associated gastric carcinogenesis among A-bomb survivors. First, candidate genes were selected by custom oligonucleotide array, developed by us, which

TABLE VI - RELATION BETWEEN VERSICAN OR OSTEONECTIN EXPRESSION AND CLINICOPATHOLOGIC CHARACTERISTICS OF GASTRIC CANCER

Variable	Versican			Osteonectin		
	Diffuse positive (%)	Focal positive or negative	p value ¹	Diffuse positive (%)	Focal positive or negative	p value ¹
Sex						
Male	30 (49)	31	0.7	16 (26)	45	0.8
Female	25 (45)	30		13 (24)	42	
Age at diagnosis						
≤65	15 (50)	15	0.8	9 (30)	21	0.5
>65	40 (47)	46		20 (23)	66	
T grade						
T1/T2	29 (37)	49	0.003	13 (17)	65	0.006
T3/T4	26 (68)	12		16 (42)	22	
N grade						
N0	18 (35)	34	0.016	7 (13)	45	0.011
N1/N2/N3	37 (58)	27		22 (34)	42	
Stage						
I/II	25 (35)	46	0.001	11 (15)	60	0.004
III/IV	30 (67)	15		18 (40)	27	
Lauren classification						
Intestinal	27 (38)	45	0.008	17 (24)	55	0.7
Diffuse	28 (64)	16		12 (27)	32	
Exposure status (all cases)						
Exposed	23 (36)	41	0.009	9 (14)	55	0.005
Nonexposed	32 (62)	20		20 (38)	32	
Exposure status (Stage I/II cases)						
Exposed	8 (22)	28	0.026	2 (6)	34	0.024
Nonexposed	17 (49)	18		9 (26)	26	
Exposure status (Stage III/IV cases)						
Exposed	15 (54)	13	0.023	7 (25)	21	0.013
Nonexposed	15 (88)	2		11 (65)	6	
Exposure status (intestinal type of Lauren classification)						
Exposed	9 (26)	26	0.054	5 (25)	30	0.097
Nonexposed	18 (49)	19		12 (65)	25	
Exposure status (diffuse type of Lauren classification)						
Exposed	14 (48)	15	0.003	4 (14)	25	0.011
Nonexposed	14 (93)	1		8 (53)	7	

¹Fisher's exact test.

TABLE VII - MULTIVARIATE LOGISTIC REGRESSION ANALYSIS OF CLINICOPATHOLOGIC CHARACTERISTICS AND EXPRESSION OF VERSICAN AND OSTEONECTIN

Variable	Hazard ratio	95% CI ¹	χ ²	p value
Sex				
Male	1	Reference	0.505	0.5
Female	0.733	0.311-1.728		
Age at diagnosis (years)				
≤65	1	Reference	1.225	0.3
>65	0.553	0.194-1.579		
T grade				
T1/2	1	Reference	0.438	0.5
T3/4	0.624	0.154-2.523		
N grade				
N0	1	Reference	2.266	0.1
N1/2/3	2.373	0.770-7.310		
Stage				
I/II	1	Reference	1.054	0.3
III/IV	2.315	0.466-11.495		
Lauren classification				
Intestinal	1	Reference	1.284	0.3
Diffuse	1.814	0.647-5.084		
Versican expression				
Diffuse positive	1	Reference	10.141	0.002
Focal positive or negative	4.484	1.783-11.364		
Osteonectin expression				
Diffuse positive	1	Reference	10.205	0.001
Focal positive or negative	6.452	2.053-20.408		

¹Exposed vs. nonexposed GC.

was applied to freshly collected cancer tissue specimens from 3 survivor patients exposed to atomic-radiation as well as 20 nonexposed patients for comparison. Second, of these candidate genes, we marked out *VCAN* (encoding versican) and *SPARC* (encoding osteonectin) genes, and their protein expression was further investigated by immunohistochemical analysis with formalin-fixed and paraffin-embedded archival cancer tissue specimens from 116 survivor patients comprised of 64 exposed and 52 nonexposed cases. In our study, we found that versican and osteonectin are expressed at significantly lower levels in tumor-associated stromas of exposed patients than in nonexposed patients. Because IR is a carcinogen and can increase an individual's risk of developing cancer, analysis of early-stage GC rather than late-stage GC is important to understand the development of radiation-induced cancer. It is important to note that the clinicopathologic, phenotypic and proliferative characteristics of the early-stage (Stage I/II) GCs analyzed in our study did not differ significantly between exposed and nonexposed patients, indicating that the GC samples analyzed in our study were collected in an unbiased manner. In Stage I/II GCs, versican and osteonectin were expressed at much lower levels in tumor-associated stromas of exposed patients than in nonexposed patients. Similar results were obtained in Stage III/IV GCs. Furthermore, multivariate logistic regression analysis revealed that reduced expression of versican and osteonectin were independent markers for GCs from exposed patients. These findings suggest that tumor-stroma interaction may be altered in the development of GCs in exposed patients, typically as demonstrated by decreased expression of versican and osteonectin in tumor-associated stromas.

In our study, stromal expression of both versican and osteonectin was lower in GCs from exposed patients than in GCs from

nonexposed patients. Because transforming growth factor (TGF)- β 1 can induce expression of both versican and osteonectin in cultured fibroblasts,^{36,37} genes associated with TGF- β signaling pathway may be altered in exposed patients. Mice with a fibroblast-specific knockout of the TGF- β Type-II receptor rapidly develop epithelial tumors,³⁸ suggesting that TGF- β receptor in fibroblasts may be altered in exposed patients.

Stromal expression of both versican and osteonectin correlates with tumor progression. In our study, stromal expression of versican and osteonectin correlated with tumor stage in GC. Versican and osteonectin were expressed less frequently in stroma of exposed patients than in nonexposed patients. Phenotypic analysis revealed that although the frequency of G-type GC decreased with advancing tumor stage in nonexposed patients, the frequency of G-type GC increased with advancing tumor stage in exposed patients. In Stage III/IV GC, a marginally significant difference was observed between the frequency of G-type GC in exposed patients and that in nonexposed patients. These findings suggest the molecular mechanism of GC progression may also differ between exposed and nonexposed patients. It has been reported that tumor stage of GC is quite comparative between exposed and nonexposed patients.³⁹ In the present study, clinicopathologic characteristics of patients including tumor stage did not statistically differ between exposed and nonexposed patients. In addition, multivariate logistic regression analysis revealed that expression of versican and osteonectin was not significant independent marker for tumor stage. Taken together, expression of versican and osteonectin may not be involved deeply in tumor progression in GC. The biologic significance of decreased expression of versican and osteonectin in tumor progression should be investigated in detail.

Versican represses cell adhesion and promotes proliferation, migration and invasion.^{10,11} Osteonectin enhances the invasive capacity of prostate and breast cancer cells.^{17,18} Therefore, prognosis of exposed patients with GC may be favorable; however, it has been reported that the excess relative risk per Gy is 1.20 for mortality,⁶ suggesting that stromal expression of versican or osteonectin dose not contribute significantly to aggressiveness of GC. Other molecules may be involved in poor prognosis of exposed patients with GC.

In the present study, strong and extensive staining of both versican and osteonectin were observed in tumor-associated stroma. It has been reported that both versican and osteonectin are components of the ECM. In breast cancer, the induction of versican secretion by fibroblasts isolated from normal and cancer tissues has been reported.¹² Expression of *SPARC* mRNA in liver myofibroblasts has been demonstrated by *in situ* hybridization.⁴⁰ In the present study, in addition to extracellular staining, intracellular

staining of versican and osteonectin in fibroblasts were observed. Furthermore, GC cells were negative for versican and osteonectin. Taken together, these results indicate that versican and osteonectin observed in tumor-associated stroma are produced mainly by tumor-associated stromal cells.

One weak point of our study is that the A-bomb radiation doses of exposed patients with GC analyzed by oligonucleotide array were low. In addition, only 3 GCs from exposed patients were analyzed by oligonucleotide array in the present study. Analysis of additional GCs is needed. In the present study, diffuse-type GC was found more frequently in exposed patients than in nonexposed patients although the difference was not statistically significant. The diffuse-type GC contains scirrhous-type GC, which is characterized by extensive fibrous stroma, infiltrative and rapid growth and poor prognosis. Because cancer stromal cells are a mixture of fibroblasts, smooth muscle cells, endothelial cells, vascular pericytes, mesenchymal stem cells and so on, difference of cell types composing cancer stroma between A-bomb exposed and nonexposed patients should be investigated.

Although expression of *TKT*, *THBS2*, *PDGFRB* and *RNASE1* was significantly lower in GC from exposed patients than in GC from nonexposed patients by oligonucleotide array, immunoreactivities for these proteins were present in GC from exposed patients. Among 6 antibodies used in the present study, the specificity of antibodies against versican and osteonectin has been characterized in detail. In contrast, the specificity of antibodies against transketolase, THBS-2, PDGF receptor- β and ribonuclease A has not been characterized in detail. Therefore, it is possible that inconsistent results between oligonucleotide array and immunostaining represent insufficient specificity of these antibodies. Immunohistochemical analysis of these proteins by specific antibodies should be performed in the near future.

In conclusion, we found significant reduction of stromal expression of versican and osteonectin in GCs from exposed patients. Although it is unclear whether all of the GCs from exposed patients were radiation-induced cancers, versican and osteonectin may be markers for radiation-associated GC. Studies of tumor-associated stromal cells rather than tumor cells may be important to elucidate the precise long-term effects of radiation exposure.

Acknowledgements

We thank Ms. Emiko Hisamoto for excellent technical assistance and advice. This work was carried out with the kind cooperation of the Research Center for Molecular Medicine, Faculty of Medicine, Hiroshima University. We also thank the Analysis Center of Life Science, Hiroshima University for the use of their facilities.

References

1. Thompson DE, Mabuchi K, Ron E, Soda M, Tokunaga M, Ochikubo S, Sugimoto S, Ikeda T, Terasaki M, Izumi S, Preston DL. Cancer incidence in atomic bomb survivors, part II: solid tumors, 1958–1987. *Radiat Res* 1994;137:S17–67.
2. Takeshima Y, Seyama T, Bennett WP, Akiyama M, Tokuoka S, Inai K, Mabuchi K, Land CE, Harris CC. p53 mutations in lung cancers from non-smoking atomic-bomb survivors. *Lancet* 1993;342:1520–1.
3. Takahashi K, Eguchi H, Arihiro K, Ito R, Koyama K, Soda M, Cologne J, Hayashi Y, Nakata Y, Nakachi K, Hamatani K. The presence of BRAF point mutation in adult papillary thyroid carcinomas from atomic bomb survivors correlates with radiation dose. *Mol Carcinog* 2007;46:242–8.
4. Yasui W, Oue N, Kitadai Y, Nakayama H. Recent advances in molecular pathobiology of gastric carcinoma. In: Kaminishi M, Takubo K, Mafune K, eds. *The diversity of gastric carcinoma pathogenesis: diagnosis, and therapy*. Tokyo: Springer, 2005:51–71.
5. Ushijima T, Sasako M. Focus on gastric cancer. *Cancer Cell* 2004;5:121–5.
6. Preston DL, Shimizu Y, Pierce DA, Suyama A, Mabuchi K. Studies of mortality of atomic bomb survivors. Report 13: solid cancer and noncancer disease mortality: 1950–1997. *Radiat Res* 2003;160:381–407.
7. Iwamoto KS, Mizuno T, Tokuoka S, Mabuchi K, Seyama T. Frequency of p53 mutations in hepatocellular carcinomas from atomic bomb survivors. *J Natl Cancer Inst* 1998;90:1167–8.
8. Schwartz NB, Pirok EW, 3rd, Mensch JR, Jr., Domowicz MS. Domain organization, genomic structure, evolution, and regulation of expression of the aggrecan gene family. *Prog Nucleic Acid Res Mol Biol* 1999;62:177–225.
9. Rahmani M, Wong BW, Ang L, Cheung CC, Carthy JM, Walinski H, McManus BM. Versican: signaling to transcriptional control pathways. *Can J Physiol Pharmacol* 2006;84:77–92.
10. Yang BL, Zhang Y, Cao L, Yang BB. Cell adhesion and proliferation mediated through the G1 domain of versican. *J Cell Biochem* 1999;72:210–20.
11. Ricciardelli C, Russell DL, Ween MP, Mayne K, Suwiwat S, Byers S, Marshall VR, Tilley WD, Horsfall DJ. Formation of hyaluronan- and versican-rich pericellular matrix by prostate cancer cells promotes cell motility. *J Biol Chem* 2007;282:10814–25.
12. Ricciardelli C, Brooks JH, Suwiwat S, Sakko AJ, Mayne K, Raymond WA, Seshadri R, LeBaron RG, Horsfall DJ. Regulation of stromal versican expression by breast cancer cells and importance to relapse-free survival in patients with node-negative primary breast cancer. *Clin Cancer Res* 2002;8:1054–60.

13. Ricciardelli C, Mayne K, Sykes PJ, Raymond WA, McCaul K, Marshall VR, Horsfall DJ. Elevated levels of versican but not decorin predict disease progression in early-stage prostate cancer. *Clin Cancer Res* 1998;4:963-71.
14. Yan Q, Sage EH. SPARC, a matricellular glycoprotein with important biological functions. *J Histochem Cytochem* 1999;47:1495-506.
15. Koukourakis MI, Giatromanolaki A, Brekken RA, Sivridis E, Gatter KC, Harris AL, Sage EH. Enhanced expression of SPARC/osteonectin in the tumor-associated stroma of non-small cell lung cancer is correlated with markers of hypoxia/acidity and with poor prognosis of patients. *Cancer Res* 2003;63:5376-80.
16. Infante JR, Matsubayashi H, Sato N, Tonascia J, Klein AP, Riall TA, Yeo C, Iacobuzio-Donahue C, Goggins M. Peritumoral fibroblast SPARC expression and patient outcome with resectable pancreatic adenocarcinoma. *J Clin Oncol* 2007;25:319-25.
17. Jacob K, Webber M, Benayahu D, Kleinman HK. Osteonectin promotes prostate cancer cell migration and invasion: a possible mechanism for metastasis to bone. *Cancer Res* 1999;59:4453-7.
18. Briggs J, Chamboredon S, Castellazzi M, Kerry JA, Bos TJ. Transcriptional upregulation of SPARC, in response to c-Jun overexpression, contributes to increased motility and invasion of MCF7 breast cancer cells. *Oncogene* 2002;21:7077-91.
19. Theocharis AD, Vynios DH, Papageorgakopoulou N, Skandalis SS, Theocharis DA. Altered content composition and structure of glycosaminoglycans and proteoglycans in gastric carcinoma. *Int J Biochem Cell Biol* 2003;35:376-90.
20. Maeng HY, Song SB, Choi DK, Kim KE, Jeong HY, Sakaki Y, Furihata C. Osteonectin-expressing cells in human stomach cancer and their possible clinical significance. *Cancer Lett* 2002;184:117-21.
21. Sobin LH, Wittekind CH, eds. TNM classification of malignant tumors, 6th edn. New York: Wiley-Liss, 2002.65-8.
22. Lauren P. The two histological main types of gastric carcinoma: diffuse and so-called intestinal-type carcinoma. An attempt at a histoclinical classification. *Acta Pathol Microbiol Scand* 1965;64:31-49.
23. Yasui W, Oue N. Systematic collection of tissue specimens and molecular pathological analysis of newly diagnosed solid cancers among atomic bomb survivors. *Int Congr Ser* 2007;1299:81-6.
24. Preston DL, Pierce DA, Shimizu Y, Cullings HM, Fujita S, Funamoto S, Kodama K. Effect of recent changes in atomic bomb survivor dosimetry on cancer mortality risk estimates. *Radiat Res* 2004;162:377-89.
25. Nagao K, Togawa N, Fujii K, Uchikawa H, Kohno Y, Yamada M, Miyashita T. Detecting tissue-specific alternative splicing and disease-associated aberrant splicing of the PTCH gene with exon junction microarrays. *Hum Mol Genet* 2005;14:3379-88.
26. Oue N, Hamai Y, Mitani Y, Matsumura S, Oshimo Y, Aung PP, Kuraoka K, Nakayama H, Yasui W. Gene expression profile of gastric carcinoma: identification of genes and tags potentially involved in invasion, metastasis, and carcinogenesis by serial analysis of gene expression. *Cancer Res* 2004;64:2397-405.
27. Hasegawa S, Furukawa Y, Li M, Satoh S, Kato T, Watanabe T, Katagiri T, Tsunoda T, Yamaoka Y, Nakamura Y. Genome-wide analysis of gene expression in intestinal-type gastric cancers using a complementary DNA microarray representing 23,040 genes. *Cancer Res* 2002;62:7012-17.
28. Inoue H, Matsuyama A, Mimori K, Ueo H, Mori M. Prognostic score of gastric cancer determined by cDNA microarray. *Clin Cancer Res* 2002;8:3475-9.
29. Zembutsu H, Ohnishi Y, Tsunoda T, Furukawa Y, Katagiri T, Ueyama Y, Tamaoki N, Nomura T, Kitahara O, Yanagawa R, Hirata K, Nakamura Y. Genome-wide cDNA microarray screening to correlate gene expression profiles with sensitivity of 85 human cancer xenografts to anticancer drugs. *Cancer Res* 2002;62:518-27.
30. Mizoshita T, Tsukamoto T, Nakanishi H, Inada K, Ogasawara N, Joh T, Itoh M, Yamamura Y, Tatematsu M. Expression of Cdx2 and the phenotype of advanced gastric cancers: relationship with prognosis. *J Cancer Res Clin Oncol* 2003;129:727-34.
31. Bode-Lesniewska B, Dours-Zimmermann MT, Odermatt BF, Briner J, Heitz PU, Zimmermann DR. Distribution of the large aggregating proteoglycan versican in adult human tissues. *J Histochem Cytochem* 1996;44:303-12.
32. Tatematsu M, Tsukamoto T, Inada K. Stem cells and gastric cancer: role of gastric and intestinal mixed intestinal metaplasia. *Cancer Sci* 2003;94:135-41.
33. Kushima R, Muller W, Stolte M, Borchard F. Differential p53 protein expression in stomach adenomas of gastric and intestinal phenotypes: possible sequences of p53 alteration in stomach carcinogenesis. *Virchows Arch* 1996;428:223-7.
34. Endoh Y, Tamura G, Ajioka Y, Watanabe H, Motoyama T. Frequent hypermethylation of the hMLH1 gene promoter in differentiated-type tumors of the stomach with the gastric foveolar phenotype. *Am J Pathol* 2000;157:717-22.
35. Motoshita J, Oue N, Nakayama H, Kuraoka K, Aung PP, Taniyama K, Matsusaki K, Yasui W. DNA methylation profiles of differentiated-type gastric carcinomas with distinct mucin phenotypes. *Cancer Sci* 2005;96:474-9.
36. Sakko AJ, Ricciardelli C, Mayne K, Tilley WD, Lebaron RG, Horsfall DJ. Versican accumulation in human prostatic fibroblast cultures is enhanced by prostate cancer cell-derived transforming growth factor beta1. *Cancer Res* 2001;61:926-30.
37. Reed MJ, Vernon RB, Abrass IB, Sage EH. TGF-beta 1 induces the expression of type I collagen and SPARC, and enhances contraction of collagen gels, by fibroblasts from young and aged donors. *J Cell Physiol* 1994;158:169-79.
38. Bhowmick NA, Chytil A, Plieth D, Gorska AE, Dumont N, Shappell S, Washington MK, Neilson EG, Moses HL. TGF-beta signaling in fibroblasts modulates the oncogenic potential of adjacent epithelia. *Science* 2004;303:848-51.
39. Suehiro S, Nagasue N, Abe S, Ogawa Y, Sasaki Y. Carcinoma of the stomach in atomic bomb survivors. A comparison of clinicopathologic features to the general population. *Cancer* 1986;57:1894-8.
40. Le Bail B, Faouzi S, Boussarie L, Guirouilh J, Blanc JF, Carles J, Bioulac-Sage P, Balabaud C, Rosenbaum J. Osteonectin/SPARC is overexpressed in human hepatocellular carcinoma. *J Pathol* 1999;189:46-52.

Immunohistochemical analysis of Reg IV in urogenital organs: Frequent expression of Reg IV in prostate cancer and potential utility as serum tumor marker

TETSUTARO HAYASHI^{1,2}, AKIO MATSUBARA², SHINYA OHARA^{1,2}, KOJI MITA²,
YASUHISA HASEGAWA², TSUGURU USUI², KOJI ARIHIRO³, SHINICHI NORIMURA¹,
KAZUHIRO SENTANI¹, NAOHIDE OUE¹ and WATARU YASUI¹

Departments of ¹Molecular Pathology, ²Urology, Hiroshima University Graduate School of Biomedical Sciences;
³Department of Anatomical Pathology, Hiroshima University Hospital, Hiroshima, Japan

Received June 25, 2008; Accepted August 26, 2008

DOI: 10.3892/or_00000194

Abstract. Regenerating islet-derived family, member 4 (Reg IV) is a candidate marker for cancer and inflammatory bowel disease and is associated with neuroendocrine and intestinal differentiation. We have reported that 14% of prostate cancer (PCa) cases are positive for Reg IV by immunohistochemistry. In the present study, we performed immunohistochemical analysis of Reg IV in other major urological cancers, including 101 renal cell carcinoma (RCC), and 95 urothelial carcinoma (UC) of urinary bladder by immunohistochemistry. We also investigated neuroendocrine differentiation by chromogranin A and synaptophysin staining along with intestinal differentiation by MUC2 staining. Immunohistochemical analysis of Reg IV revealed no expression of Reg IV in RCC, and only one case (1%) of UC expressed Reg IV. Neither neuroendocrine nor intestinal differentiation was found in RCC. Among 95 UC cases, neuroendocrine differentiation was detected in 13 cases (14%), and intestinal differentiation was observed in 33 cases (35%). In one Reg IV-positive UC case, MUC2 staining was observed. Since Reg IV expression was frequently found in PCa, we also measured Reg IV levels in sera from patients with PCa by enzyme-linked immunosorbent assay. The serum Reg IV concentration in PCa patients (n=38, mean \pm SE, 1.69 \pm 0.16 ng/ml) was significantly higher than that in control individuals (n=40, 1.28 \pm 0.11 ng/ml, P=0.0199, Mann-Whitney U test). The sensitivity and specificity for detection of PCa were 34% (13/38) and 90% (36/40), respectively. These results suggest that among

major urologic cancers, Reg IV is expressed frequently in PCa, and that serum Reg IV represents a novel biomarker for PCa.

Introduction

Prostate cancer (PCa) is one of the most common types of cancer and is the second leading cause of cancer death among men in the United States (1). Currently, the standard diagnostic marker for PCa is prostate-specific antigen (PSA) and the rapid incorporation of aggressive PSA testing has resulted in dramatically earlier identification of PCa (2). However, the significantly high false-positive rate of PSA combined with its widespread clinical application, has lead to a tremendous increase in the number of unnecessary prostate biopsies (3). Therefore, there has been an increasing emphasis in the need to determine multiple protein biomarkers for use in the diagnosis and prognosis of PCa.

Renal cell carcinoma (RCC) accounts for ~2% of all human cancers worldwide, and in 2000 189,000 cases and 91,000 deaths were reported (4). RCC is characterized by an absence of early warning signs leading to a rather high percentage of advanced, metastatic tumors upon diagnosis. For example, the classic triad of pain, hematuria, and a palpable flank mass is encountered in only 10% of patients and is usually associated with the presence of advanced disease (5). Unlike other solid malignancies in which established serum or urinary biomarkers are available for early detection, relatively few diagnostic tools are currently available for the early detection of renal tumors. Therefore, an ideal tumor marker with high sensitivity and specificity offers the ideal opportunity for early detection of RCC.

Bladder cancer, the majority of which is urothelial carcinoma (UC) is the sixth most common cancer in the world. A distinctive feature of UC is that multiple metachronous or synchronous cancers frequently develop, arising from either a polyclonal origin or metastasis from a single clone. Thus, bladder cancer patients need a long-term follow-up with repeated urine cytology and cystoscopy for monitoring. Conventional urine cytology has been the standard non-invasive method for cancer detection and disease monitoring.

Correspondence to: Dr Wataru Yasui, Department of Molecular Pathology, Hiroshima University Graduate School of Biomedical Sciences, 1-2-3 Kasumi, Minami-ku, Hiroshima 734-8551, Japan
E-mail: wyasui@hiroshima-u.ac.jp

Key words: regenerating islet-derived family member 4, serum tumor marker, prostate cancer